NASA Reference Publication 1220

1989

Hot-Jet Simulation in Cryogenic Wind Tunnels

Keisuke Asai
Langley Research Center
Hampton, Virginia

NASA
National Aeronautics and Space Administration
Office of Management
Scientific and Technical Information Division

Abstract

In order to evaluate hot-jet simulation capabilities in cryogenic wind tunnel testing, simple theoretical calculations have been performed. The similarity parameters, isentropic flow properties, and normal shock relations were calculated for a variety of jet simulation techniques. The results were compared with those estimated for a full-scale flight condition. It has been shown that cryogenic wind tunnel testing provides an opportunity for the most accurate hot-jet simulation. By using compressed nitrogen gas at ambient or moderately elevated temperatures as a jet gas, almost all the relevant similarity parameters, including the jet temperature and velocity ratios and the Reynolds numbers, could be set to full-scale flight values. The only exception was the ratio of specific heats for jet flow. In an attempt to match the ratio of specific heats for the turbojet flow, gases other than pure nitrogen were considered. It was found that a nitrogen and methane mixture at moderately elevated temperatures behaved like the real combustion gas. With this mixture used as a jet gas, complete simulation of the full-scale turbojet exhaust became possible in cryogenic wind tunnels.

Introduction

One of the major advances made in modern transonic wind tunnel testing is the cryogenic wind tunnel technology developed at the NASA Langley Research Center (refs. 1 and 2). A cryogenic wind tunnel provides us with unique testing capabilities. One is the achievement of full-scale flight Reynolds numbers with a reasonable power requirement. Another is the separation of the effects of Reynolds number, Mach number, and dynamic pressure (aeroelasticity). Through the use of these testing capabilities, significant improvements in aerodynamic simulation can be attained.

However, a number of factors still remain which interfere with accurate aerodynamic prediction. Wall and support interference effects are among the major problems. The simulation of jet exhaust effects is also important, particularly when propulsion-airframe integration is essential in the aircraft design.

In wind tunnel testing, complete simulation of the full-scale turbojet exhaust has been practically impossible. The most common method is to use compressed air at ambient temperatures to simulate the actual jet nozzle pressure ratio. With a cold jet, however, one fails to simulate the jet-temperature-related effects, which have been reported as being important in some critical aerodynamic problems. Of course, testing techniques which use heated gas are available today, but they are not used in routine tests because of their complexity. We should also note that even if a miniature turbojet engine is used to simulate a hot jet, the problem associated with the Reynolds number gap still remains.

For jet simulation it is not essential that the absolute jet temperature be duplicated, but the relative value of jet temperature to free-stream temperature should be duplicated. This requirement implies that it is possible in cryogenic wind tunnels to simulate hot-jet exhaust with gas at ambient or moderately elevated temperatures because the working gas in a cryogenic wind tunnel is nitrogen as cold as 100 K. In contrast with the previous hot-jet simulation techniques, simulation at the full-scale Reynolds number becomes practical in cryogenic wind tunnels. The coupling of the jet temperature effects and the Reynolds number effects may be very significant in a complicated flow field containing separated flows and shock waves.

This potential capability of cryogenic wind tunnel testing has not been emphasized in the previous studies. In this report some simple theoretical considerations are presented to evaluate the accuracy of hot-jet simulation in cryogenic wind tunnels. For different jet simulation techniques, values of the similarity parameters, flow properties undergoing isentropic expansions, and flow properties through normal shocks are calculated. The results are then compared with those estimated for a full-scale flight condition. The effects of the ratio of specific heats for the jet gas are also discussed, and a testing technique which uses a mixture of nitrogen and methane is proposed to correct the ratio of specific heats for a simulated jet exhaust.

Symbols and Abbreviations

A	sectional area, m^2
a	sound velocity, m/sec
C_D	drag coefficient
c_p	specific heat at constant pressure, kJ/kg-K
c_v	specific heat at constant volume, kJ/kg-K
d	diameter, m
h	specific enthalpy, kJ/kg
k	thermal conductivity, J/m-sec-K
L	linear dimension, m
M	Mach number; molecular weight
N_{Pr}	Prandtl number

N_{Re}	Reynolds number
p	pressure, bar
R	gas constant, kJ/kg-K
T	temperature, K
t	time, sec
V	velocity, m/sec
x	mole fraction
Z	compressibility factor
β	boattail angle, deg
γ	ratio of specific heats, c_p/c_v
μ	dynamic viscosity, Pa-sec
ρ	density, kg/m^3
Subscripts:	
AFT	afterbody
amb	ambient
i	i-component in gas mixture
j	jet exhaust
max	maximum
ref	ideal gas with $\gamma = 1.4$
t	stagnation
0	free stream
1	upstream of normal shock
2	downstream of normal shock
∞	free stream
Superscript:	
*	sonic
Abbreviations:	
C/P	combustion products
c.p.	critical point
NPR	nozzle pressure ratio
STA	fuselage station
t.p.	triple point

Similarity Parameters

An interacting flow field of the jet exhaust and the external flow is considered here. As is well-known, wind tunnel tests are always conducted on the basis of the similarity rule (ref. 3). If we assume that the flow field is governed by the Navier-Stokes equation system (conservation equations of mass, momentum, and energy), it is easy to derive similarity parameters by nondimensionalizing the equations.

We assume here that the gas is thermally perfect but not necessarily calorically perfect. Thus, the specific heat at constant pressure c_p is a function of temperature only. We also assume that the viscosity is a function of temperature only, as is the thermal conductivity. All the gases considered in this report except cryogenic nitrogen gas meet these assumptions.

A number of similarity parameters are introduced from the nondimensionalized equations. Among them, the following four parameters are generally considered the most important:

Reynolds number, $N_{\mathrm{Re}} = \rho V L/\mu$

Mach number, $M = V/a$

Ratio of specific heats, $\gamma = c_p/c_v$

Prandtl number, $N_{\mathrm{Pr}} = \mu c_p/k$

In wind tunnel testing, these four similarity parameters should be matched to the flight values in both external and jet internal flows. However, matching these eight parameters is not sufficient for proper simulation of the flow field, because the external flow and the jet flow are not independent of each other in the interacting (mixing) region. To account for the effects of these interactions, new similarity parameters should be introduced. These parameters are derived not from the field equations but from the boundary condition.

The boundary condition in the interacting flow region can be written in generalized form as

$$f((p,T,V)_{\mathrm{ext}},(p,T,V)_{\mathrm{int}}) = 0 \qquad (1)$$

where the subscripts ext and int represent the values for the external flow and the jet internal flow. Note that this equation may include spatial and temporal derivatives such as $\partial p/\partial x$ and $\partial T/\partial t$.

By nondimensionalizing this equation, we obtain a new set of scaling parameters. Actually, they are the ratios of internal reference values to values for the external flow:

Geometrical scale ratio, L_j/L_0

Pressure ratio, p_j/p_0

Temperature ratio, T_j/T_0

Velocity ratio, V_j/V_0

where the subscripts 0 and j indicate the external flow (free stream) and the internal flow (jet exhaust). Consequently, the similarity parameters relevant to jet simulation testing are summarized as follows:

Group 1 (simulation of external flow):

$M_0; N_{\mathrm{Re},0}; \gamma_0; N_{\mathrm{Pr},0}$

Group 2 (simulation of internal flow):

$M_j; N_{\mathrm{Re},j}; \gamma_j; N_{\mathrm{Pr},j}$

Group 3 (simulation of interaction):

$p_j/p_0; T_j/T_0; V_j/V_0; L_j/L_0$

For most tests, L_j/L_0 is equal to unity since it is usual that the same scaling is adopted for both internal and external geometries.

For cryogenic nitrogen, the parameters such as the ratio of specific heats and the Prandtl number are not valid similarity parameters because cryogenic nitrogen is not thermally perfect and the viscosity and the heat conductivity are functions of both pressure and temperature. In the early stages of the development of cryogenic wind tunnels, the real-gas effects of cryogenic nitrogen were thoroughly studied (refs. 4 to 6). It has been proved that real-gas effects are negligible for most practical tests in cryogenic wind tunnels, as long as the pressure is no greater than 9 bars. In other words, cryogenic nitrogen actually behaves like an ideal diatomic gas, even if the real values for the ratio of specific heats and the Prandtl number deviate from the ideal values ($\gamma = 1.4$ and $N_{\mathrm{Pr}} = 0.72$).

Previous Jet Simulation Techniques and Jet Temperature Effects

So far, a jet simulation technique which uses compressed dry air at ambient temperature has been the most common in wind tunnel testing. This technique simulates the correct nozzle pressure ratio but fails to simulate the jet-temperature-related effects. That is, jet temperature ratio, jet velocity ratio, and the ratio of specific heats for a simulated jet are quite different from the actual values for turbojet exhaust flow.

Figure 1 summarizes the aerodynamic problems in which the jet-temperature-related effects are considered critical. The most well-known problem is the nozzle afterbody drag at transonic Mach numbers (refs. 7 to 10). The effect of a thrust reverser is also very sensitive to jet temperature (ref. 11). Aerodynamics of V/STOL airplanes in proximity to the ground is one of the major problems in which simulation of the jet temperature effects is indispensable (ref. 12).

The previous studies on jet temperature effects were carried out mainly at the NASA Langley Research Center (LaRC) and the USAF Arnold Engineering Development Center (AEDC), with emphasis on the transonic afterbody drag (refs. 7 to 10). The pressure drag acting on the nozzle afterbody at transonic Mach numbers can be very sensitive to jet temperature, particularly in the presence of separation.

There are two distinguishable effects of the jet temperature on afterbody flow: (1) the effect of γ on plume shape and (2) the effect of T_j/T_0 or V_j/V_0 or both on jet entrainment. These two factors sometimes have conflicting effects on the afterbody drag, and this conflict makes prediction of the transonic afterbody drag more difficult. In some cases, the use of cold air results in a measured value of afterbody drag 20 percent above the correct value (refs. 7 and 8).

Figure 2 illustrates the hot-jet simulators used at LaRC and AEDC. At LaRC, a hydrogen peroxide (H_2O_2) technique was used to generate hot-jet exhaust (ref. 8). In this technique, the exhaust gas is a mixture of steam and oxygen. Temperatures as high as 1000 K are attainable. It should be noted that the composition of the mixture is quite different from that of the real turbojet exhaust.

On the other hand, the researchers at AEDC utilized the combustion of ethylene with air to represent hot-jet exhaust (refs. 9 and 10). Unlike the H_2O_2 technique, properties of the combustion products of ethylene are similar to those of the actual turbojet exhaust gas. The maximum temperature attained is 1800 K.

These techniques provide us with solutions to the jet temperature effects. However, they require a very complicated model (water-cooled in some cases) and a sophisticated control and instrument system. Even the wind tunnel structure may need insulation. The tests become very costly and special attention should be paid to the safety of the tests.

For these practical reasons, previous studies have concentrated on the determination of good correlation parameters which can correct the effects of jet temperature on afterbody drag. However, for a highly three-dimensional flow field including shock–boundary-layer interactions, it does not seem probable to isolate a critical correlation parameter and to predict hot-jet results from cold-jet model tests. For these critical problems, complete simulation of hot-jet exhausts in wind tunnel tests is indispensable.

Analysis

Modeling Thermodynamic Properties of Gases

In this report we consider several kinds of gases, including the actual turbojet exhaust gas. All the gases except cryogenic nitrogen are thermally perfect in the pressure and temperature ranges considered in this analysis. For example, figure 3 shows the variations of pressure and temperature in the simulated jet flow of nitrogen. The curves for the compressibility factor, $Z = 0.99$ and 1.01, and the saturation boundary are also indicated in the figure. With the assumption that γ for nitrogen gas is unchanged and equal to 1.4 during the expansion process, isentropes become a straight line. The three lines shown in figure 3 represent isentropes of a nitrogen jet from given stagnation conditions to $M = 2.0$. As is shown, nitrogen gas is thermally perfect on these isentropes. This is true for the other jet gases considered here.

For thermally perfect gases, specific heats are functions of temperature only. The viscosity and thermal conductivity have a very weak dependence on pressure. In this analysis, we express c_p, μ, and k as the fourth-order polynomial of temperature. These approximate functions are developed through regression analysis from the values (at 1 bar) tabulated in references 13 and 14. These functions are accurate to within 0.5 percent.

For cryogenic nitrogen, c_p, γ, μ, and k are functions of both pressure and temperature. Thus, the values of γ and μ are calculated from the expressions given in reference 15. The values of c_p and k are evaluated through interpolation of the tabulated values in references 13 and 16.

Thermodynamic Properties of Gas Mixtures

The actual turbojet combustion gas and the decomposed gas of hydrogen peroxide are mixtures of several gas components. In this report, we also deal with a mixture of nitrogen and methane having a different mole ratio.

If all components in the mixture are thermally perfect gases, c_p for the mixture can be obtained from the values for the individual components by applying the Gibbs-Dalton law:

$$\bar{c}_p = \sum_i x_i \bar{c}_{p,i} \tag{2}$$

$$\overline{M} = \sum_i x_i \overline{M}_i \tag{3}$$

$$c_p = \bar{c}_p / \overline{M} \tag{4}$$

where x_i indicates the mole fraction of component i in the mixture. A bar indicates the value on a mole basis, and $\overline{M}$ is the equivalent molecular weight of the mixture. The viscosity and thermal conductivity of the mixture are calculated from the following empirical relationships (refs. 17 and 18):

$$\mu_{\text{mix}}^{-1/2} = \sum_i x_i (\mu_i)^{-1/2} \tag{5}$$

$$k_{\text{mix}}^{-1/2} = \sum_i x_i (k_i)^{-1/2} \tag{6}$$

When these formulas are applied to air assumed to be a mixture of O_2, N_2, CO_2, H_2O, and Ar, the estimated values of μ and k are accurate to within 2 percent.

The compositions of the turbojet combustion products and the decomposition products of hydrogen peroxide are given in the appendix.

Evaluation of Similarity Parameters

Reference condition. To evaluate the similarity parameters, we need to define the reference conditions. We assume here that the external flow (tunnel flow) is represented by the free-stream condition and that the free-stream Mach number M_0 (reference Mach number) is equal to 1.0. The reference condition for the internal flow (jet flow) is assumed to be the condition at the nozzle throat, that is, $M_j = 1.0$. In the case of a convergent nozzle, the internal reference condition is the nozzle exit condition.

Reference pressure and temperature are calculated with the assumption that gas expands isentropically from a given stagnation condition to the reference condition. For both the external and internal flows, isentropic solutions are obtained with the procedure shown in the *Isentropic Expansions* section. Thermodynamic properties such as γ, μ, and k are evaluated from the calculated values of pressure and temperature.

Datum condition. For comparison purposes, the similarity parameters for a flight condition are calculated and used as a datum. The external datum flow is assumed to have stagnation conditions of $p_{t,0} = 1.0$ bar and $T_{t,0} = 300$ K. These conditions are realized in sonic flight at an altitude of 5000 m.

The internal datum condition is evaluated with the J-79 turbojet engine (used for the F-4 Phantom, etc.) as the example. The stagnation pressure and temperature of jet exhaust at the nozzle entrance are calculated as follows (see ref. 19 for details):

$p_{t,j}/p_{t,0} = 4.0 \text{ bar}/1.0 \text{ bar} = 4.0$

$T_{t,j}/T_{t,0} = 1000 \text{ K}/300 \text{ K} = 3.33$ (non-afterburning)

We assume the turbojet exhaust gas to be the combustion products of n-octane (C_8H_{18}) with air. The composition of the combustion gas is given in the appendix.

Isentropic Expansions

To examine the simulation accuracy of various jet simulation techniques, the variations of flow properties in isentropic expansions are calculated for various gases assuming one-dimensional flow for simplicity. First, we consider that gas is neither thermally perfect nor calorically perfect (e.g., cryogenic nitrogen). In this case, the compressibility factor Z is not unity but varies with pressure and temperature. The ratio of specific heats γ is also a function of pressure and temperature.

For the isentropic process, the first law of thermodynamics can be expressed in the following form:

$$dh = \rho^{-1}\, dp = (ZRT/p)\, dp \tag{7}$$

or

$$h_t - h = -R \int_{p_t}^{p} (ZT/p)\, dp \tag{8}$$

Integration in equation (8) should be carried out along a path satisfying the following relationship:

$$\frac{dT}{dp} = \frac{\gamma - 1}{\gamma} \frac{Z - p(\partial Z/\partial p)_T}{Z + T(\partial Z/\partial T)_p} \frac{T}{p} \tag{9}$$

From the conservation of energy for adiabatic flow, the velocity can be expressed as

$$V^2 = 2(h_t - h) \tag{10}$$

Thus the Mach number is

$$M = V/a \tag{11}$$

where a is the speed of sound obtained from

$$a^2 = \frac{Z^2}{Z - p(\partial Z/\partial p)_T} \gamma RT \tag{12}$$

The first calculations for the real-gas effects associated with isentropic flow of cryogenic nitrogen were carried out at NASA Langley Research Center (ref. 4) with the Jacobsen et al. equation of state for nitrogen (ref. 16). See reference 4 for the detailed solution procedure.

For a thermally perfect gas (all the jet gases treated in this report are in this category), the fundamental equations for isentropic flow are much simpler. Thus,

$$h_t - h = -R \int_{p_t}^{p} (T/p)\, dp \tag{13}$$

Integration in equation (13) should be made along a path satisfying the following equation:

$$\frac{dT}{dp} = \frac{\gamma - 1}{\gamma} \frac{T}{p} \tag{14}$$

or

$$p = p_t \exp\left[\int_{T_t}^{T} \frac{\gamma\, dT}{(\gamma - 1)T}\right] \tag{15}$$

In this analysis, numerical integrations in equations (13) and (15) are carried out with the trapezoid rule.

Mach number is obtained from

$$M = [2(h_t - h)/\gamma RT]^{1/2} \tag{16}$$

When $M_0 = 1.0$ and $p_{t,j}/p_{t,0} = 4.0$, the jet flow expands to Mach number M_j of about 2.0. Thus, the calculations are made over a range of Mach numbers up to $M_j = 2.5$.

Normal Shock Relations

In general, jet flow expanding into the ambient low-pressure condition contains oblique shocks and Mach disks. In order to assess the simulation accuracy, the variations of flow properties through a normal shock are calculated for each jet simulation testing technique.

Across a normal shock, the conservation equations for mass, momentum, and energy are satisfied as follows:

$$\rho_1 V_1 = \rho_2 V_2 \tag{17}$$

$$p_1 + \rho_1 V_1^2 = p_2 + \rho_2 V_2^2 \tag{18}$$

$$h_1 + (V_1^2/2) = h_2 + (V_2^2/2) \tag{19}$$

where upstream and downstream quantities are indicated by the subscripts 1 and 2, respectively.

For real gases, the thermal equation of state is $p_2 = f(\rho_2, T_2)$ and the caloric equation of state is $h_2 = f(\rho_2, T_2)$. In order to solve these equations for the flow parameters downstream of the shock with a given upstream condition, an iterative procedure should be used. The detailed solution procedure is outlined in reference 4.

For thermally perfect gases, the normal shock solutions can be obtained readily. Thus,

$$h(T_2) = h(T_1) + (V_1^2/2) - (V_2/V_1)^2(V_1^2/2) \quad (21)$$

$$T_2 = \left[p_1/(\rho_1 V_1^2) + 1 - (V_2/V_1)\right](V_2/V_1)V_1^2/R \quad (22)$$

where the specific enthalpy $h(T)$ is expressed as a polynomial function because $dh(T) = c_p(T)\ dT$ and $c_p(T)$ is given in the form of the fourth-order polynomial function, as described previously.

Thus, substituting equation (21) into equation (20), we obtain the tenth-order algebraic equation with respect to V_2/V_1; this equation is numerically solved for V_2/V_1 using the secant method in this analysis. The other flow parameters, such as p_2/p_1, are obtained from the calculated value of V_2/V_1 and the given upstream quantities. Normal shock solutions are obtained over a range of the upstream Mach numbers M_1 from 1.0 to 2.5.

Results and Discussions

Comparison of Similarity Parameters

The similarity parameters were evaluated for a variety of jet simulation techniques designated as cases A to I. Case A represents calculations of a flight condition which is used as a datum in assessing the simulation accuracy for wind tunnel testing techniques. Case B is a jet simulation technique in atmospheric wind tunnels with compressed cold air as a jet gas. Case C is a conventional hot-jet simulation technique in atmospheric tunnels using hydrogen peroxide to generate hot-jet exhausts. Cases D to F and cases G to I represent hot-jet simulation techniques in cryogenic wind tunnels at atmospheric and elevated pressures, respectively. In these cases, compressed nitrogen gas at ambient or moderately elevated temperatures is used as a jet gas.

The calculated values of the similarity parameters are presented in table 1. To assess the simulation capability of each technique, the tabulated values of similarity parameters are normalized by the parameters estimated for the flight condition (case A). We assume that the model is 10 percent scale.

Figure 4 shows the simulation capabilities for various jet simulation techniques. The polygon shown in figure 4 is composed of the normalized similarity parameters. The closer the polygon is to a complete circle (corresponding to the actual flight condition, case A), the more accurate the simulation is.

Case A′ in figure 4(a) represents wind tunnel testing with a miniature turbojet engine (hypothetical) in a conventional atmospheric wind tunnel. With this technique, simulation of jet-temperature-related effects is perfect, but the Reynolds number is much smaller (10 percent) than the full-scale flight value. If we use this technique, the only way to increase the test Reynolds number is to increase the model size.

A testing technique using compressed air (case B) has several deficiencies. The jet temperature effects are not simulated correctly with this technique. The temperature and velocity ratios are much smaller than the actual values while the ratio of specific heats is slightly larger than that for the turbojet exhaust. In addition, the Reynolds number is very small in both the external and internal flows. We should note that the jet Reynolds number is large compared with that for the external flow because jet flow is cold (another jet-temperature-related effect). This difference implies that even if the free-stream Reynolds number is set to the full-scale value by pressurizing the tunnel, the jet Reynolds number will become erroneously large. Then the jet profile at the nozzle exit will be quite different from the actual jet flow. The jet exit profile is a very important parameter affecting the interaction between the jet flow and the external flow.

With a hot-jet simulation technique using hydrogen peroxide (case C), simulation of the jet temperature effects is possible but not complete. Although the actual jet temperature ratio is duplicated, the velocity ratio becomes larger than the actual value since the decomposed gases of hydrogen peroxide (steam and oxygen) are lighter than the combustion products. Moreover, the ratio of specific heats becomes smaller than the actual value, which will introduce an error because of overcorrection of the jet plume shape. The jet Prandtl number, which is a measure of the ability of gas to convert kinetic energy into heat, is also incorrect. The large difference in Prandtl numbers may have a measurable effect on the jet mixing. As in case A′, the Reynolds number problem cannot be solved with this technique.

Figures 4(b) and 4(c) are the results for hot-jet simulation techniques using nitrogen jet at ambient or moderately elevated temperatures in cryogenic wind tunnels (cases D to I). As is shown clearly in these figures, the temperature and velocity ratios of flight can be matched in cryogenic wind tunnels. Of all the jet-temperature-related effects, only the ratio of specific heats of the jet is larger (by a small amount) than the correct value since pure nitrogen is used as the test gas for jet flow.

It should be emphasized that with a hot-jet simulation technique in cryogenic wind tunnels, the test Reynolds number can be increased to the full-scale value merely by pressurizing the tunnel moderately (2.0 to 4.0 bars). As shown in figure 4(c), all the parameters can be set very close to actual flight

values in pressurized cryogenic wind tunnels (cases H to I). This is not the case for the other hot-jet simulation techniques which use heated gas for jet exhaust (cases A′ and B). This capability is one of the greatest advantages of the use of cryogenic wind tunnels for hot-jet simulation.

As the jet temperature decreases from 500 K (case I) to 333 K (case G), the Reynolds number for the internal flow deviates from the actual value (fig. 4(c)). This is because of the nonlinear variation of the Reynolds number with temperature. (The Reynolds number varies approximately as $(T/T_{\text{amb}})^{-1.4}$.) For Reynolds number simulation, case I ($p_{t,0} = 4.0$ bar and $T_{t,0} = 150$ K) is the best of all the cases in figure 4. In case I, all the similarity parameters except γ_j are very close to the actual flight values. The effect of incorrect γ in simulated jet flow is discussed in the following section.

We should note that in cryogenic wind tunnels, the values of γ and N_{Pr} for the free stream are not the correct values (case A). However, as was previously discussed, cryogenic nitrogen behaves like an ideal diatomic gas even if the real values of γ and N_{Pr} are different from the ideal values ($\gamma = 1.4$ and $N_{\text{Pr}} = 0.72$). These deviations in γ and N_{Pr} do not cause any simulation errors (refs. 4 to 6).

Effects of γ on Simulated Jet Flow

In the previous section, we found that all the similarity parameters except the ratio of specific heats for jet flow can be matched to the flight values in pressurized cryogenic wind tunnel testing. The ratio of specific heats is a very important parameter for compressible flows. For jet flows it determines a jet plume shape, one of the major factors affecting the transonic afterbody flow. In this section, we discuss the effects of incorrect γ on the flow properties of simulated jet flow.

The calculated flow parameters in one-dimensional isentropic expansions for various jet simulation techniques are shown in figures 5 and 6. The abscissa shows a local Mach number to which gas expands from a given stagnation condition. The ordinate in figures 6(a) to 6(e) indicates the value of isentropic flow parameters normalized by the value for an ideal diatomic gas ($\gamma = 1.4$). For comparison purposes, the curves for the real combustion gas are also shown in the figures as dashed lines.

Figure 5 shows the variation of γ with Mach number in simulated jet flows and real turbojet exhaust gas. Since the turbojet combustion gas is not calorically perfect, its γ varies with Mach number or temperature. Contrary to this condition, the values of γ for compressed air (case B) and nitrogen gas (cases G to I) are practically constant and have a value of 1.4. These gases are therefore both calorically and thermally perfect over the range of pressures and temperatures considered. The testing technique using hydrogen peroxide (case C) matches the Mach number variation for the turbojet exhaust gas. However, the value of γ in this case is much smaller than the value for the real gas throughout the range.

Figures 6(a) to 6(e) show the variations in isentropic flow parameters for cases B, C, and G to I. The effects of incorrect γ are clearly shown in these figures. Among the isentropic parameters plotted in figure 6, the stream-tube area ratio A/A^* is a good measure to assess the effects of γ on the jet plume shape. For the jet simulation tests using compressed air or nitrogen (figs. 6(a) and 6(c) to 6(e)), the plume diameter becomes smaller than that of the actual jet exhaust, the result being the underestimation of the blockage effect of jet flow. On the other hand, the decomposed gas of hydrogen peroxide (fig. 6(b)) has a larger plume diameter than the real exhaust gas. This increased plume diameter means that the blockage (source) effect would be overestimated with this technique even if the jet entrainment (sink) effect were correctly simulated.

Figures 7(a) to 7(e) are the normal shock solutions obtained for cases B, C, and G to I. The abscissa in these figures shows the Mach number upstream of the normal shock, and the ordinate indicates the ratio of downstream flow properties to upstream values normalized by the same ratio for an ideal diatomic gas. The dashed lines in the figures represent curves for the real turbojet exhaust gas.

Similar to the results for isentropic expansions, large errors due to incorrect γ are shown in the normal shock relations. The flow properties downstream of the shock are quite different from those obtained for the actual turbojet exhaust. Since a supersonic jet contains a complex system of shock waves, the incorrect value of γ can have a strong effect on the entire flow structure of the jet flow.

Generally, the effect of γ is small in subsonic jets. This means that jet flow can be simulated with pure nitrogen if the nozzle pressure ratio is small enough. On the contrary, when the jet is supersonic an error resulting from incorrect γ is too large to be ignored. It may be possible to compensate for the effect of incorrect γ by adjusting the pressure ratio by a small amount as we do in the tests using cold air. However, for such a critical problem as the transonic nozzle afterbody drag with separated flow, the correct value of γ must be duplicated in wind tunnel testing.

Use of Methane to Correct γ

In order to simulate the real values for γ for the turbojet gas, we must reduce the value of γ for the

simulated jet flow. To reduce γ, the use of polyatomic gas is required.

Table 2 is taken from the table originally given in reference 20. We also appended some gases which are not listed in the original table but which are considered suitable for use in cryogenic wind tunnels. Generally, polyatomic gas has a higher boiling point than diatomic gas. So the use of polyatomic gas decreases the advantage of cryogenic wind tunnel testing.

Among all the candidate gases, methane gas was selected for further study because methane has a relatively low boiling point (111.6 K at 1.0 bar), and therefore we can make full use of the high Reynolds number capability of cryogenic wind tunnels. Ethylene is not suitable since its boiling point at 1.0 bar is 169.4 K. Methane is a nontoxic gas, and it is inexpensive and easy to purchase. The thermodynamic characteristics of methane are thoroughly documented in reference 21.

Figure 8 shows the variations of pressure and temperature in simulated jet flow of pure methane. The dashed lines indicate curves for the compressibility factor $Z = 0.99$ and 1.01. The saturation boundary is also indicated. The three straight lines in figure 8 represent isentropic expansions of methane from different stagnation conditions to $M = 2.0$ for γ constant and equal to 1.3. As shown, methane is thermally perfect on these isentropes. Because γ for methane is smaller than that for the turbojet exhaust, we deal with a mixture of nitrogen and methane instead of pure methane.

In tables 3(a) to 3(c), the calculated values of similarity parameters are presented for pressurized cryogenic wind tunnel testing with a mixture of nitrogen and methane as a jet gas. These calculations were made by varying the mole fraction of methane from 0 to 50 or 60 percent in 10-percent increments.

Since γ is smaller for methane than for nitrogen, the value of γ decreases with the increasing mole fraction of methane. Thus, we can adjust the value of γ for the simulated jet by changing the amount of methane in the mixture. The mole fraction of methane required to obtain the correct value of γ decreases with increasing jet temperature as follows:

Jet temperature, K	Mole fraction of methane, percent
333	60
417	40
500	30

For cases I to I-3 ($T_{t,j} = 500$ K), the variations of γ in isentropic expansions are shown in figure 9. The mole fraction of methane ranges from 0 (case I) to 30 percent (case I-3). For pure nitrogen, the value of γ is constant and equal to 1.4. As the amount of methane increases, the curve for γ approaches the dashed line (representing the real combustion gas). At the mole ratio of 30 percent, the variation of γ completely coincides with the actual turbojet combustion gas. Note that γ of a mixture of nitrogen and methane varies with the Mach number (temperature) as the real turbojet exhaust gas does. This variation is because methane is not calorically perfect in this range of temperatures.

The polygonal plots of the normalized similarity parameters are shown in figures 10(a) to 10(c). Again, the model is assumed to be 10 percent scale. As shown in these figures, the increase in the mole fraction of methane results in errors in the velocity ratio because the molecular weight of methane is less than that of nitrogen. In this respect, cases G-6 ($T_{t,j} = 333$ K) and H-4 ($T_{t,j} = 417$ K) are not so accurate as case I-3 ($T_{t,j} = 500$ K), since the mole fraction of methane required to obtain the correct γ_j increases as the jet temperature decreases.

For case I-3, all the similarity parameters including γ_j are matched to the actual flight values, as is shown in figure 10(c). The jet Reynolds number is also very close to the full-scale value.

The calculated values of isentropic flow parameters for a mixture of nitrogen and methane are shown in figures 11(a) to 11(c) (corresponding to cases G-6, H-4, and I-3). The normal shock solutions are also shown in figures 12(a) to 12(c). As shown in these figures, the flow properties agree very well with the results for the turbojet exhaust gas for Mach numbers up to 2.0. The results for case I-3 (figs. 11(c) and 12(c)) are practically identical to those for the real turbojet exhaust gas up to $M_j = 2.5$. Case I-3 can therefore be considered to be the best of all the jet simulation techniques treated in this report, although it requires the elevation of the jet gas temperature to 500 K.

Conclusions

In order to evaluate hot-jet simulation capabilities in cryogenic wind tunnel testing, simple theoretical calculations have been performed. The similarity parameters, isentropic flow properties, and normal shock relations were calculated for a variety of jet simulation techniques. The results were then compared with those estimated for a full-scale flight condition. The general conclusions drawn from this study can be summarized as follows:

1. In cryogenic wind tunnels, hot-jet exhaust can be simulated with gases at ambient or moderately elevated temperatures.

2. In contrast with conventional jet simulation techniques, this hot-jet method simulates most of the relevant similarity parameters, including the jet temperature and velocity ratios and the Reynolds numbers.

3. When compressed nitrogen gas is used as a jet gas, the ratio of specific heats for the simulated jet flow becomes slightly larger than the actual turbojet value. This increased specific heat ratio causes noticeable error in supersonic jet simulation.

4. We can adjust the ratio of specific heats for the simulated jet flow to the actual value for the turbojet exhaust by using a specified mole ratio of nitrogen and methane. This mixture behaves like the real combustion gas in isentropic expansions and through normal shocks.

5. Through use of a nitrogen-methane mixture at moderately elevated temperatures as a jet gas, complete simulation of the full-scale turbojet exhaust becomes possible in cryogenic wind tunnels.

6. A hot-jet simulation technique which uses a cryogenic environment will provide a testing tool to solve some critical aerodynamic problems, such as transonic afterbody drag, thrust-reverser use, and V/STOL aerodynamics, in which complete simulation of hot-jet exhausts is necessary. This technique can also be applied to the testing of jet engine nozzle system performance as well as to the testing of hot-jet reingestion.

NASA Langley Research Center
Hampton, VA 23665-5225
June 8, 1989

Appendix

Compositions of Turbojet Combustion Products and Decomposed Hydrogen Peroxide

Turbojet Exhaust Gas

We consider here the complete combustion of n-octane, C_8H_{18}, supplied at 298 K with oxygen:

$$2C_8H_{18} + 25O_2 \longrightarrow 16CO_2 + 18H_2O$$

The composition of the combustion products can be obtained from the conservation of energy through the combustion process (ref. 19):

Enthalpy of the reactants = Enthalpy of the products

In this analysis, effects of dissociation are neglected, since the maximum temperature in the cycle is lower than 1500 K.

Assuming that dry air is supplied at 700 K and the combustion product gases leave the combustion chamber at 1400 K, we obtain the following values:

Component	Mole fraction
CO_2	0.0390
H_2O	.0435
N_2	.7639
O_2	.1445
Ar	.0091

The apparent molecular weight of the combustion gas is 28.89. The fuel-air ratio is 1.95 percent, and the percent excess air is 239 percent.

Hydrogen-Peroxide Decomposed Gas

According to reference 8, the solution of H_2O_2 with mass fraction of 0.9 (mole fraction of 0.827) is used to produce exhaust gas at 1013 K. The composition of the decomposed products is as follows:

Component	Mole fraction
H_2O	0.708
O_2	.292

The apparent molecular weight of this product is 22.10.

References

1. Goodyer, Michael J.; and Kilgore, Robert A.: The High Reynolds Number Cryogenic Wind Tunnel. AIAA Paper No. 72-995, Sept. 1972.
2. Kilgore, Robert A.; Goodyer, Michael J.; Adcock, Jerry B.; and Davenport, Edwin E.: *The Cryogenic Wind-Tunnel Concept for High Reynolds Number Testing.* NASA TN D-7762, 1974.
3. Covert, Eugene E.: Challenges Associated With High Speed, High Reynolds Number Testing in Ground Facilities. *A Collection of Technical Papers—AIAA 15th Aerodynamic Testing Conference,* May 1988, pp. 458–473. (Available as AIAA-88-2005.)
4. Adcock, Jerry B.: *Real-Gas Effects Associated With One-Dimensional Transonic Flow of Cryogenic Nitrogen.* NASA TN D-8274, 1976.
5. Adcock, Jerry B.; and Johnson, Charles B.: *A Theoretical Analysis of Simulated Transonic Boundary Layers in Cryogenic-Nitrogen Wind Tunnels.* NASA TP-1631, 1980.
6. Wagner, Bernhard: Estimation of Simulation Errors in the European Transonic Wind Tunnel (ETW). *ICAS Proceedings 1982—13th Congress of the International Council of the Aeronautical Sciences/AIAA Aircraft Systems and Technology Conference, Volume 1,* B. Laschka and R. Staufenbiel, eds., Aug. 1982, pp. 731–740. (Available as ICAS-82-5.4.3.)
7. *Aerodynamics of Aircraft Afterbody.* AGARD-AR-226, June 1986.
8. Compton, William B., III: *Effects of Jet Exhaust Gas Properties on Exhaust Simulation and Afterbody Drag.* NASA TR R-444, 1975.
9. Robinson, C. E.; High, M. D.; and Thompson, E. R.: Exhaust Plume Temperature Effects on Nozzle Afterbody Performance Over the Transonic Mach Number Range. *Airframe/Propulsion Interference,* AGARD-CP-150, Mar. 1975, pp. 19-1–19-16.
10. Peters, William Lee: A Simulation Technique for Jet Temperature Effects on Nozzle-Afterbody Drag at Transonic Mach Numbers. AIAA-85-1463, July 1985.
11. Price, Earl A., Jr.; and Peters, William L.: Test Techniques for Jet Effects on Fighter Aircraft. Wind Tunnels and Testing Techniques, AGARD-CP-348, Feb. 1984, pp. 24-1–24-17.
12. *Fluid Dynamics of Jets With Applications to V/STOL.* AGARD-CP-308, Jan. 1982.
13. L'Air Liquide, Div. Scientifique (Nissim Marshall, transl.): *Gas Encyclopaedia.* Elsevier/North-Holland Inc., c.1976.
14. Hilsenrath, Joseph; Beckett, Charles W.; Benedict, William S.; Fano, Lilla; Hoge, Harold J.; Masi, Joseph F.; Nuttall, Ralph L.; Touloukian, Yeram S.; and Woolley, Harold W.: *Tables of Thermal Properties of Gases.* NBS Circ. 564, U.S. Dep. of Commerce, Nov. 1, 1955.
15. Dress, David A.: *Computer Program for Calculating Flow Parameters and Power Requirements for Cryogenic Wind Tunnels.* NASA TM-87609, 1985.
16. Jacobsen, R. T.; Stewart, R. B.; McCarty, R. D.; and Hanley, H. J. M.: *Thermophysical Properties of Nitrogen From the Fusion Line to 3500 R (1944 K) for Pressures to 150 000 psia (10 342 × 10^5 N/m^2).* NBS Tech. Note 648, U.S. Dep. of Commerce, Dec. 1973.
17. Touloukian, Y. S.; Saxena, S. C.; and Hestermans, P.: *Viscosity. Thermophysical Properties of Matter, Volume 11,* IFI/Plenum, c.1975.
18. Touloukian, Y. S.; Liley, P. E.; and Saxena, S. C.: *Thermal Conductivity—Nonmetallic Liquids and Gases. Thermophysical Properties of Matter, Volume 3,* IFI/Plenum, 1970.
19. Bathie, William W.: *Fundamentals of Gas Turbines.* John Wiley & Sons, Inc., c.1984.
20. Pindzola, M.: *Jet Simulation in Ground Test Facilities.* AGARDograph 79, Nov. 1963.
21. Goodwin, R. D.: *The Thermophysical Properties of Methane, From 90 to 500 K at Pressures to 700 Bar.* NBS TN-653, U.S. Dep. of Commerce, Apr. 1974.

Table 1. Calculated Similarity Parameters for Various Jet Simulation Techniques

Similarity parameter	[a]Case A	[b]Case B	[c]Case C	[d]Case D	[d]Case E	[d]Case F	[e]Case G	[e]Case H	[e]Case I
Free-stream gas	Air	Air	Air	N_2	N_2	N_2	N_2	N_2	N_2
Jet gas	C/P	Air	$H_2O + O_2$	N_2	N_2	N_2	N_2	N_2	N_2
$p_{t,0}$, bar	1.0	1.0	1.0	1.0	1.0	1.0	2.0	3.0	4.0
$p_{t,j}$, bar	4.0	4.0	4.0	4.0	4.0	4.0	8.0	12.0	16.0
$T_{t,0}$, K	300	300	300	100	125	150	100	125	150
$T_{t,j}$, K	1000	300	1000	333	417	500	333	417	500
M_0	1.0	1.0	1.0	1.0	1.0	1.0	1.0	1.0	1.0
$N_{\mathrm{Re},0} \times 10^{-6}$, m^{-1}	14.6	14.6	14.6	70.3	50.6	38.7	140.8	151.9	154.7
[f]γ_0	1.40	1.40	1.40	(1.42)	(1.41)	(1.41)	(1.45)	(1.44)	(1.43)
[f]$N_{\mathrm{Pr},0}$	.72	.72	.72	(.79)	(.76)	(.76)	(.78)	(.78)	(.77)
M_j	1.0	1.0	1.0	1.0	1.0	1.0	1.0	1.0	1.0
$N_{\mathrm{Re},j} \times 10^{-6}$, m^{-1}	13.4	58.5	12.7	52.8	39.1	31.6	103.7	117.4	126.0
γ_j	1.33	1.40	1.28	1.40	1.40	1.40	1.40	1.40	1.40
$N_{\mathrm{PR},j}$	.72	.72	.89	.72	.71	.73	.72	.71	.73
L_j/L_0	1.0	1.0	1.0	1.0	1.0	1.0	1.0	1.0	1.0
p_j/p_0	4.08	4.00	4.16	3.99	4.00	4.00	3.99	4.00	3.99
T_j/T_0	3.43	1.00	3.52	3.33	3.34	3.34	3.34	3.34	3.34
V_j/V_0	1.81	1.00	2.05	1.85	1.84	1.83	1.87	1.86	1.86

[a]Corresponds to full-scale flight condition.
[b]Corresponds to atmospheric wind tunnel testing with compressed cold air as jet gas.
[c]Corresponds to atmospheric wind tunnel testing with hydrogen peroxide to represent hot jet.
[d]Corresponds to cryogenic wind tunnel testing at atmospheric pressure with compressed nitrogen as jet gas.
[e]Corresponds to cryogenic wind tunnel testing at elevated pressure with compressed nitrogen as jet gas.
[f]Parenthetical values for the cryogenic nitrogen are real values; however, their deviation from ideal values (case A) does not cause any simulation error.

Table 2. Gaseous Media Suitable for Jet Simulation Tests

Medium	T, K	p, bar	γ	R, J/kg-K	Boiling point, K
Turbojet exhaust	806		1.34	285	
Ramjet exhaust	1830		1.27	317	
Rocket exhaust	3170		1.23	377	
Helium 4	298	1.0	1.67	2080	4.22
Argon	300	1.0	1.67	208	87.29
n-hydrogen	298	1.0	1.41	4130	20.38
Air	300	1.0	1.40	287	81.74
Nitrogen	300	1.0	1.40	297	77.35
Oxygen	300	1.0	1.39	260	90.18
Carbon monoxide	300	1.0	1.40	297	81.62
Carbon dioxide	300	1.0	1.29	189	[a]194.6
Ammonia	320	1.0	1.31	488	239.7
Freon 14	298	1.0	1.15	94.3	145.2
Methane	300	1.0	1.30	517	111.6
Ethylene	298	1.0	1.24	294	169.4
Ethane	300	1.0	1.19	274	184.4
Air	1830		1.30	301	
Nitrogen	1000		1.36	297	
H_2 + Air (burning)	1440		1.29	307	
H_2 + Air (burning)	1830		1.27	317	
H_2O_2 (0.10H_2O)	1010		1.27	376	
JATO exhaust	1900		1.27	385	
LOX + JP	3270		1.24	377	

[a]Sublimation.

Table 3. Calculated Similarity Parameters for Jet Simulation Techniques in Cryogenic Wind Tunnels With Nitrogen-Methane Mixture as Jet Gas

(a) $p_{t,0}$ = 2.0 bar and $T_{t,0}$ = 100 K

Similarity parameter	[a]Case A	[b]Case G	[b]Case G-1	[b]Case G-2	[b]Case G-3	[b]Case G-4	[b]Case G-5	[b]Case G-6
Free-stream gas	Air	N_2	N_2	N_2	N_2	N_2	N_2	N_2
Jet gas	C/P	N_2	$N_2 + CH_4$ (10%)	$N_2 + CH_4$ (20%)	$N_2 + CH_4$ (30%)	$N_2 + CH_4$ (40%)	$N_2 + CH_4$ (50%)	$N_2 + CH_4$ (60%)
$p_{t,0}$, bar	1.0	2.0	2.0	2.0	2.0	2.0	2.0	2.0
$p_{t,j}$, bar	4.0	8.0	8.0	8.0	8.0	8.0	8.0	8.0
$T_{t,0}$, K	300	100	100	100	100	100	100	100
$T_{t,j}$, K	1000	333	333	333	333	333	333	333
M_0	1.0	1.0	1.0	1.0	1.0	1.0	1.0	1.0
$N_{Re,0} \times 10^{-6}$, m^{-1}	14.6	140.8	140.8	140.8	140.8	140.8	140.8	140.8
[c]γ_0	1.40	(1.45)	(1.45)	(1.45)	(1.45)	(1.45)	(1.45)	(1.45)
[c]$N_{Pr,0}$	.72	(.78)	(.78)	(.78)	(.78)	(.78)	(.78)	(.78)
M_j	1.0	1.0	1.0	1.0	1.0	1.0	1.0	1.0
$N_{Re,j} \times 10^{-6}$, m^{-1}	13.4	103.7	106.2	108.5	110.7	112.6	114.3	115.8
γ_j	1.33	1.40	1.39	1.38	1.37	1.36	1.35	1.34
$N_{PR,j}$	.72	.72	.71	.71	.70	.70	.70	.70
L_j/L_0	1.0	1.0	1.0	1.0	1.0	1.0	1.0	1.0
p_j/p_0	4.08	3.99	4.01	4.02	4.03	4.04	4.06	4.07
T_j/T_0	3.43	3.34	3.36	3.37	3.39	3.41	3.42	3.43
V_j/V_0	1.81	1.87	1.90	1.95	1.99	2.04	2.09	2.15

[a]Corresponds to full-scale flight condition.

[b]Corresponds to cryogenic wind tunnel testing with compressed nitrogen-methane mixture as jet gas.

[c]Parenthetical values for the cryogenic nitrogen are real values; however, their deviation from ideal values (case A) does not cause any simulation error.

Table 3. Continued

(b) $p_{t,0}$ = 3.0 bar and $T_{t,0}$ = 125 K

Similarity parameter	[a]Case A	[b]Case H	[b]Case H-1	[b]Case H-2	[b]Case H-3	[b]Case H-4	[b]Case H-5
Free-stream gas	Air	N_2	N_2	N_2	N_2	N_2	N_2
Jet gas	C/P	N_2	$N_2 + CH_4$ (10%)	$N_2 + CH_4$ (20%)	$N_2 + CH_4$ (30%)	$N_2 + CH_4$ (40%)	$N_2 + CH_4$ (50%)
$p_{t,0}$, bar	1.0	3.0	3.0	3.0	3.0	3.0	3.0
$p_{t,j}$, bar	4.0	12.0	12.0	12.0	12.0	12.0	12.0
$T_{t,0}$, K	300	125	125	125	125	125	125
$T_{t,j}$, K	1000	417	417	417	417	417	417
M_0	1.0	1.0	1.0	1.0	1.0	1.0	1.0
$N_{Re,0} \times 10^{-6}$, m^{-1}	14.6	151.9	151.9	151.9	151.9	151.9	151.9
[c]γ_0	1.40	(1.44)	(1.44)	(1.44)	(1.44)	(1.44)	(1.44)
[c]$N_{Pr,0}$	.72	(.78)	(.78)	(.78)	(.78)	(.78)	(.78)
M_j	1.0	1.0	1.0	1.0	1.0	1.0	1.0
$N_{Re,j} \times 10^{-6}$, m^{-1}	13.4	117.4	119.6	121.6	123.5	125.1	126.5
γ_j	1.33	1.40	1.38	1.37	1.35	1.34	1.33
$N_{PR,j}$	.72	.71	.71	.70	.70	.69	.69
L_j/L_0	1.0	1.0	1.0	1.0	1.0	1.0	1.0
p_j/p_0	4.08	4.00	4.02	4.04	4.05	4.07	4.09
T_j/T_0	3.43	3.34	3.37	3.39	3.42	3.44	3.46
V_j/V_0	1.81	1.86	1.89	1.93	1.98	2.02	2.07

[a]Corresponds to full-scale flight condition.
[b]Corresponds to cryogenic wind tunnel testing with compressed nitrogen-methane mixture as jet gas.
[c]Parenthetical values for the cryogenic nitrogen are real values; however, their deviation from ideal values (case A) does not cause any simulation error.

Table 3. Concluded

(c) $p_{t,0}$ = 4.0 bar and $T_{t,0}$ = 150 K

Similarity parameter	[a]Case A	[b]Case I	[b]Case I-1	[b]Case I-2	[b]Case I-3	[b]Case I-4	[b]Case I-5
Free-stream gas	Air	N_2	N_2	N_2	N_2	N_2	N_2
Jet gas	C/P	N_2	$N_2 + CH_4$ (10%)	$N_2 + CH_4$ (20%)	$N_2 + CH_4$ (30%)	$N_2 + CH_4$ (40%)	$N_2 + CH_4$ (50%)
$p_{t,0}$, bar	1.0	4.0	4.0	4.0	4.0	4.0	4.0
$p_{t,j}$, bar	4.0	16.0	16.0	16.0	16.0	16.0	16.0
$T_{t,0}$, K	300	150	150	150	150	150	150
$T_{t,j}$, K	1000	500	500	500	500	500	500
M_0	1.0	1.0	1.0	1.0	1.0	1.0	1.0
$N_{Re,0} \times 10^{-6}$, m^{-1}	14.6	154.7	154.7	154.7	154.7	154.7	154.7
[c]γ_0	1.40	(1.43)	(1.43)	(1.43)	(1.43)	(1.43)	(1.43)
[c]$N_{Pr,0}$	.72	(.77)	(.77)	(.77)	(.77)	(.77)	(.77)
M_j	1.0	1.0	1.0	1.0	1.0	1.0	1.0
$N_{Re,j} \times 10^{-6}$, m^{-1}	13.4	126.0	126.6	128.2	129.6	130.9	132.0
γ_j	1.33	1.40	1.37	1.35	1.33	1.31	1.30
$N_{PR,j}$	.72	.73	.71	.70	.70	.70	.70
L_j/L_0	1.0	1.0	1.0	1.0	1.0	1.0	1.0
p_j/p_0	4.08	3.99	4.03	4.06	4.08	4.11	4.13
T_j/T_0	3.43	3.34	3.38	3.41	3.44	3.47	3.50
V_j/V_0	1.81	1.86	1.88	1.92	1.96	2.01	2.05

[a]Corresponds to full-scale flight condition.
[b]Corresponds to cryogenic wind tunnel testing with compressed nitrogen-methane mixture as jet gas.
[c]Parenthetical values for the cryogenic nitrogen are real values; however, their deviation from ideal values (case A) does not cause any simulation error.

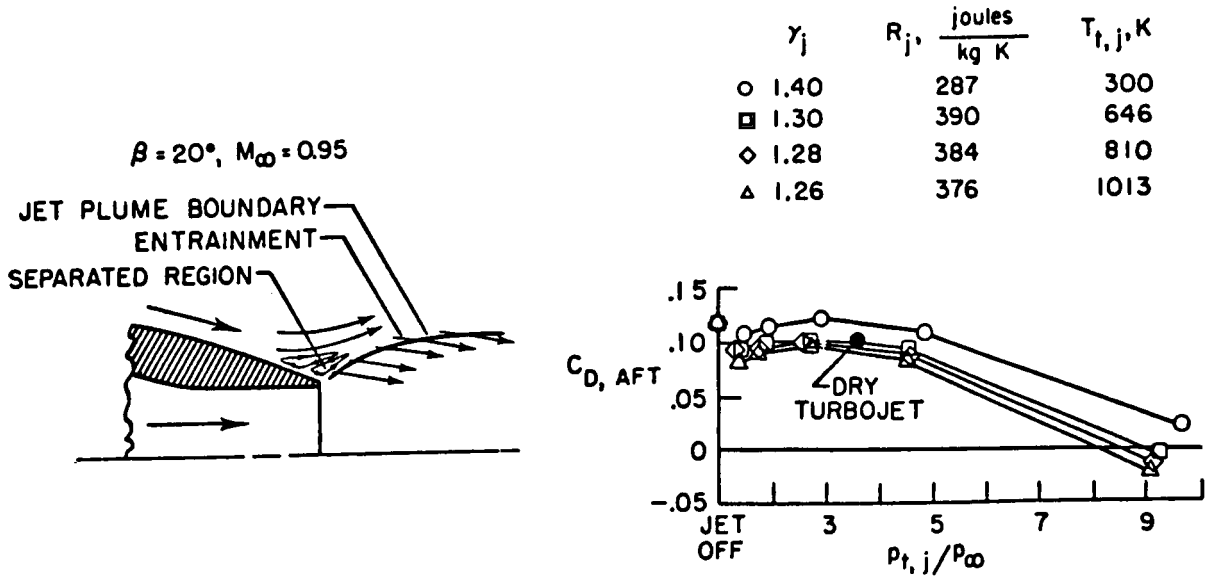

(a) Nozzle afterbody drag. (From ref. 8.)

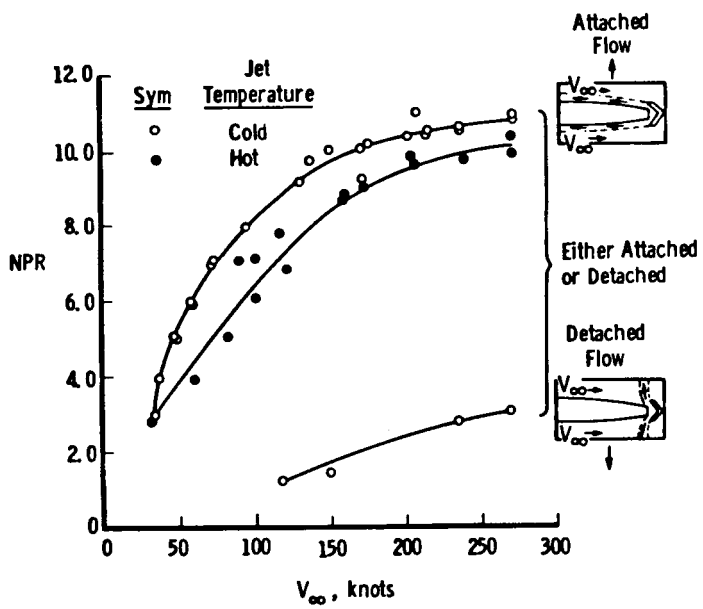

(b) Thrust reverser. (From ref. 11.)

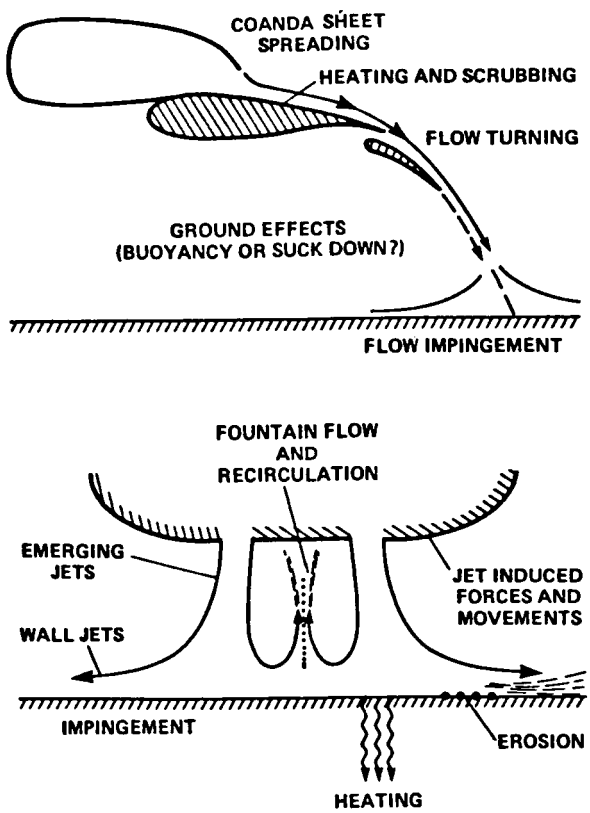

(c) V/STOL aerodynamics. (From ref. 12.)

Figure 1. Aerodynamic problems sensitive to jet-temperature-related effects.

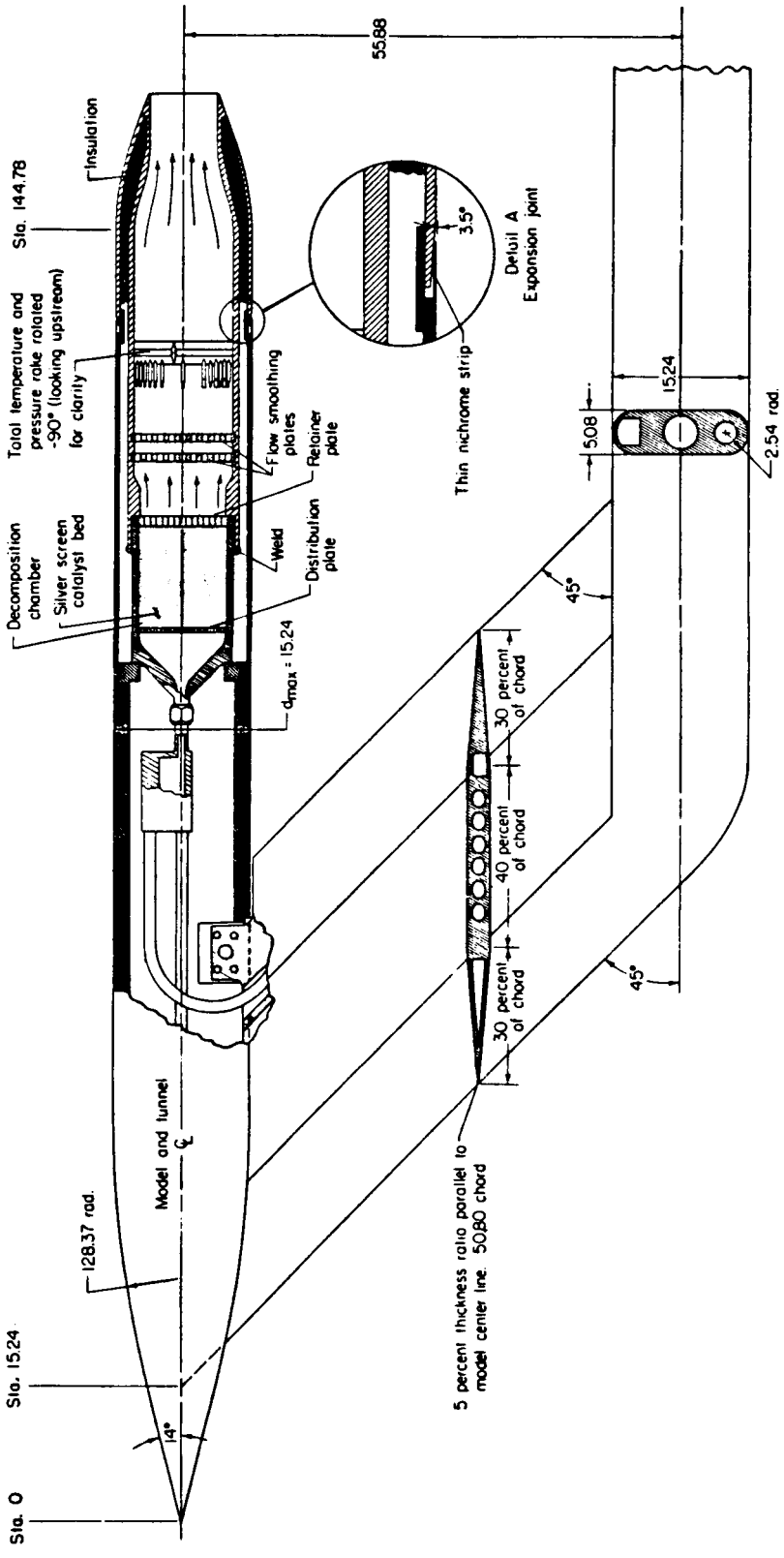

(a) Hydrogen peroxide technique. (From ref. 8.) All dimensions are in centimeters unless otherwise indicated.

Figure 2. Conventional hot-jet simulation techniques.

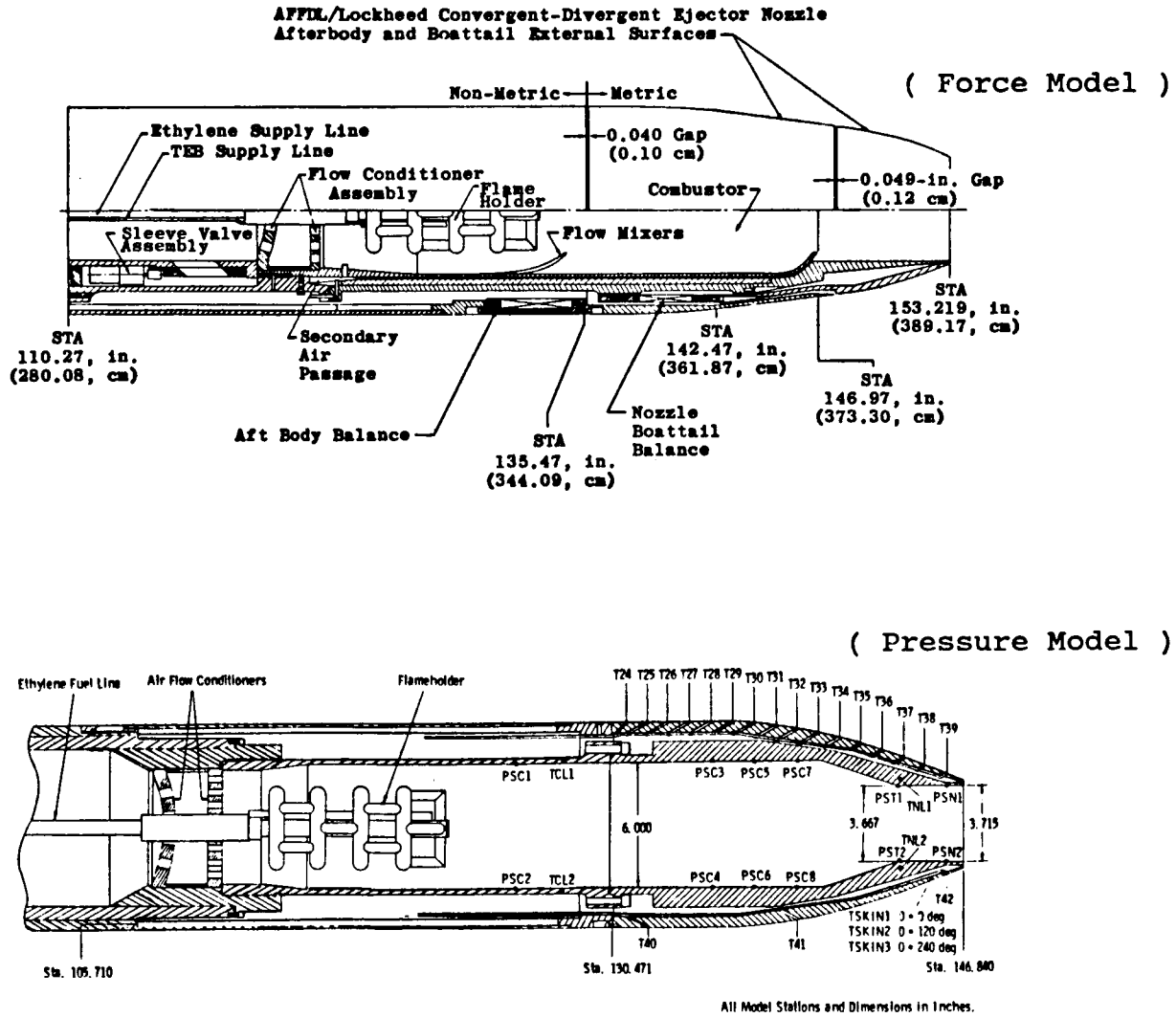

(b) Ethylene-air combustion. (From refs. 9 and 10.)

Figure 2. Concluded.

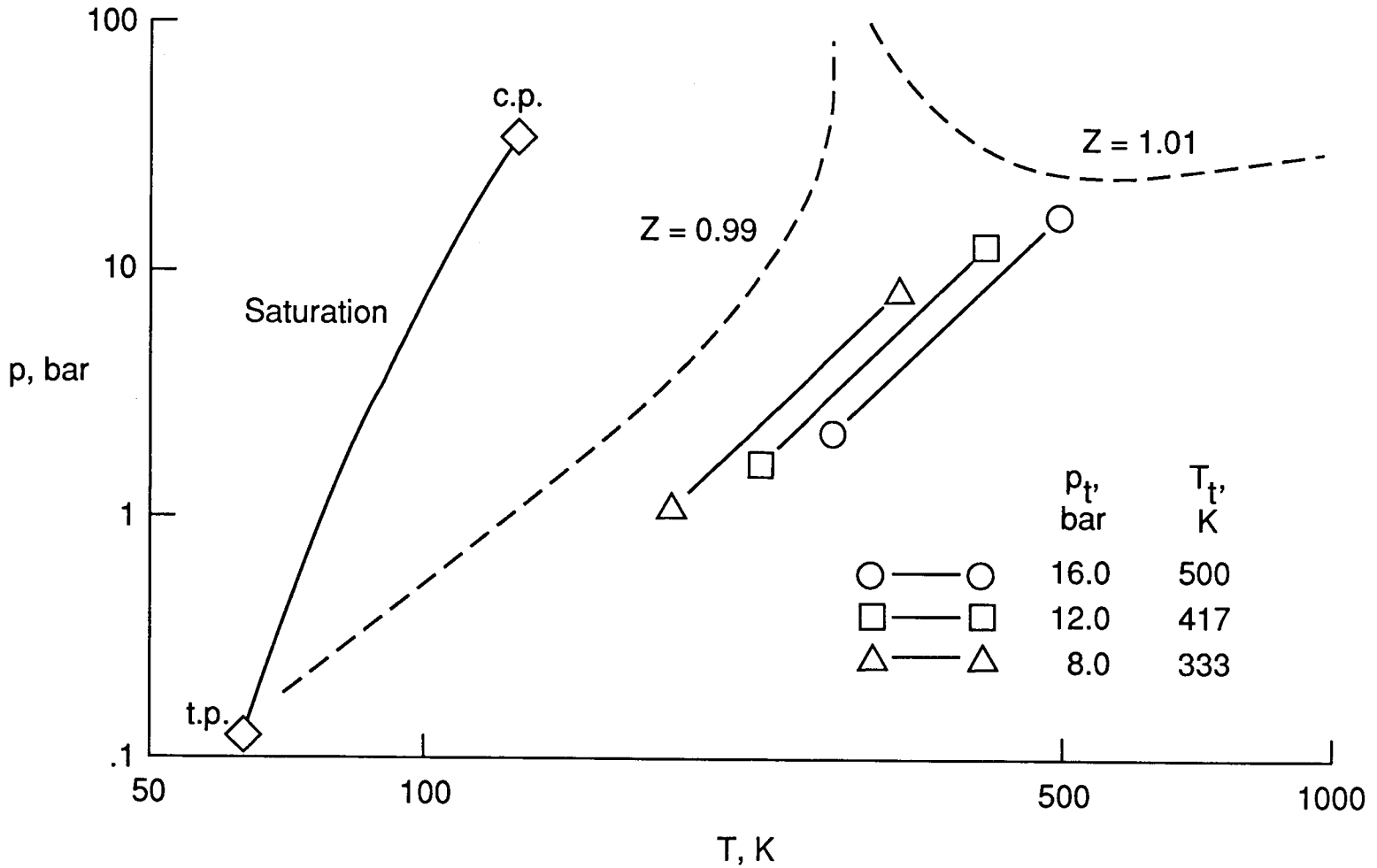

Figure 3. Isentropic expansions of nitrogen gas.

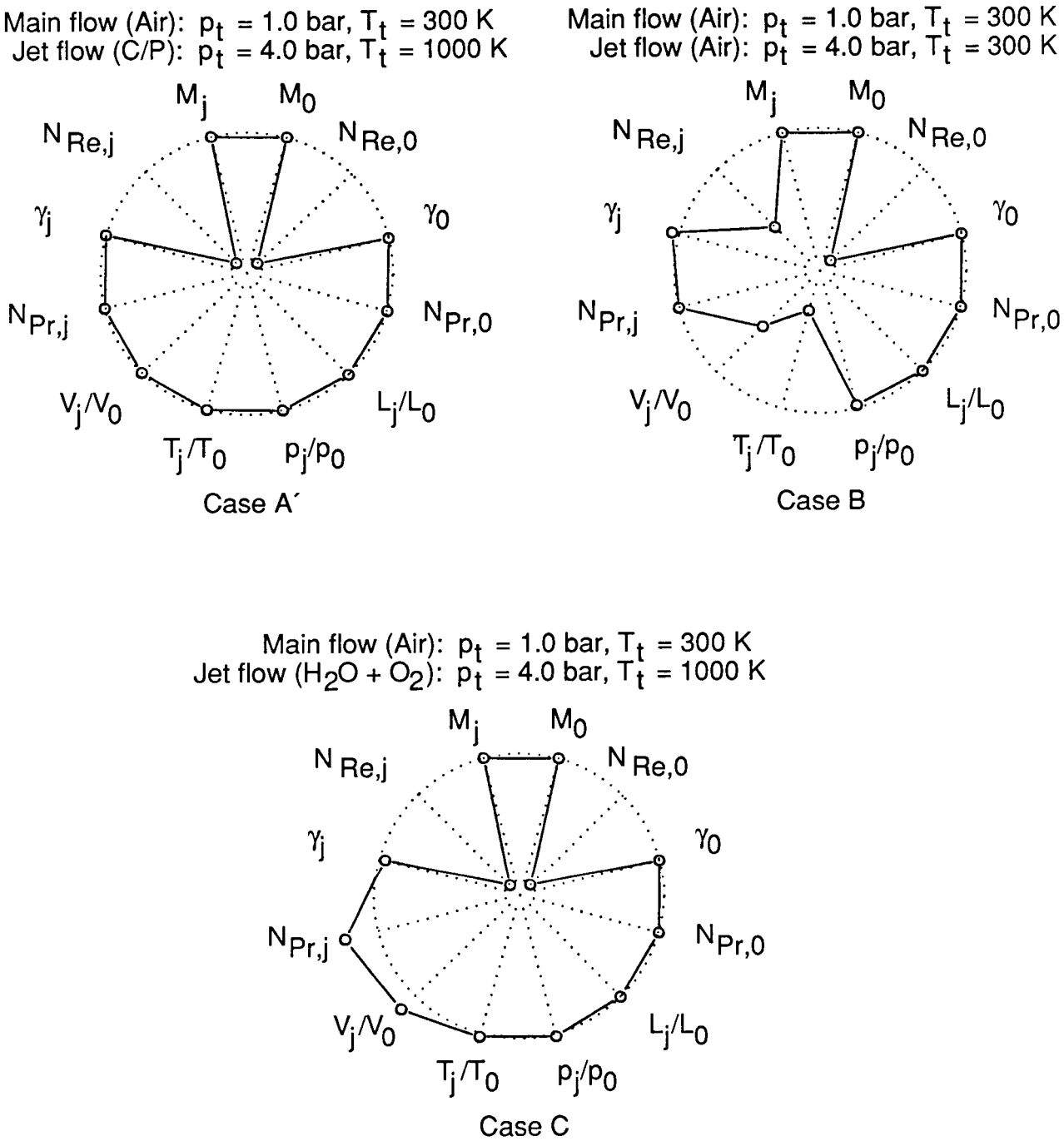

(a) Cases A′, B, and C.

Figure 4. Simulation capabilities of various jet simulation techniques.

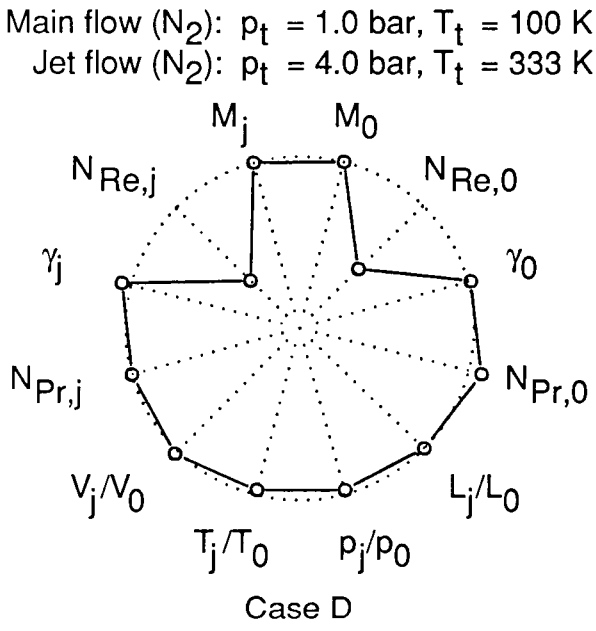

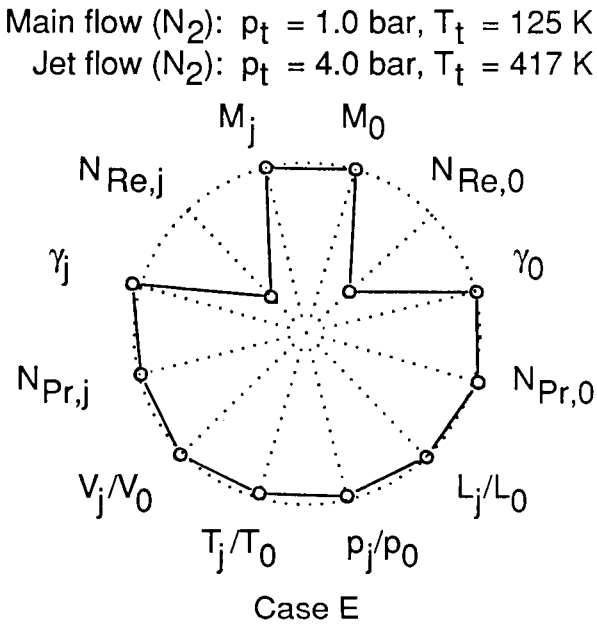

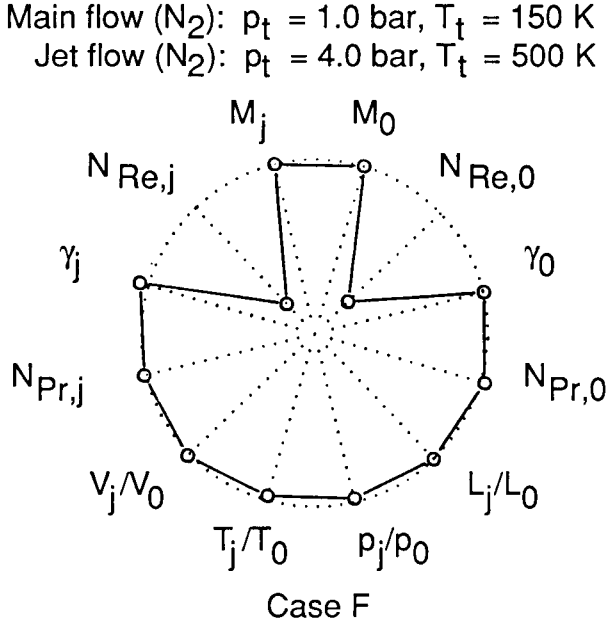

(b) Cases D, E, and F.

Figure 4. Continued.

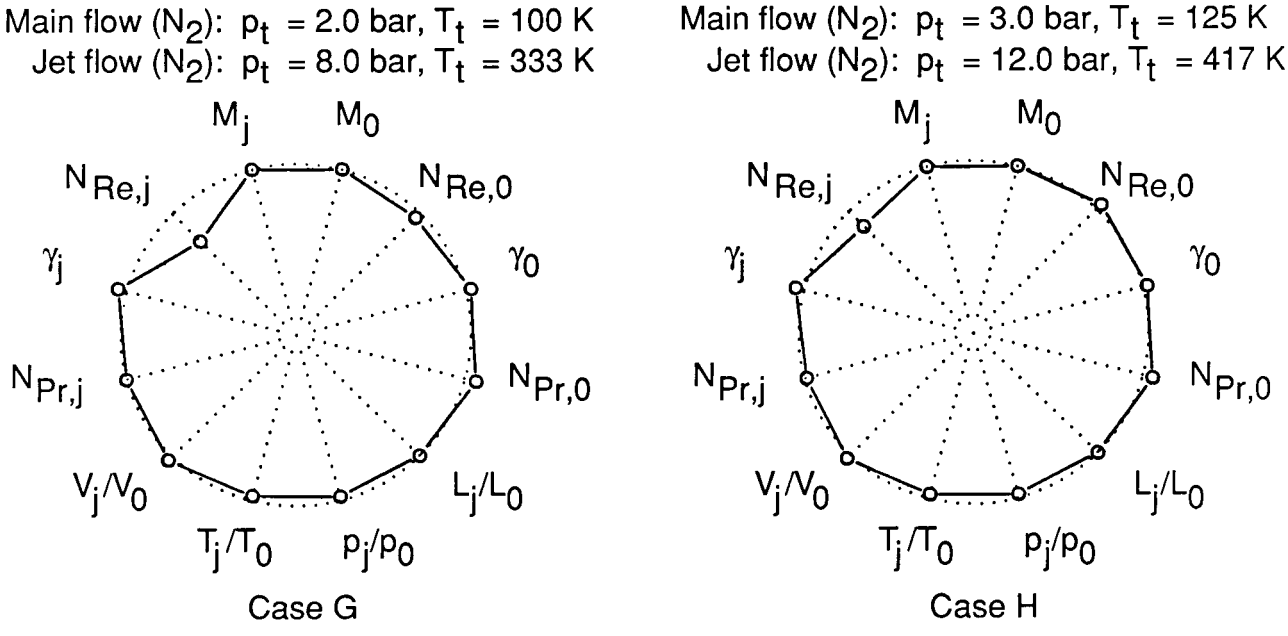

(c) Cases G, H, and I.

Figure 4. Concluded.

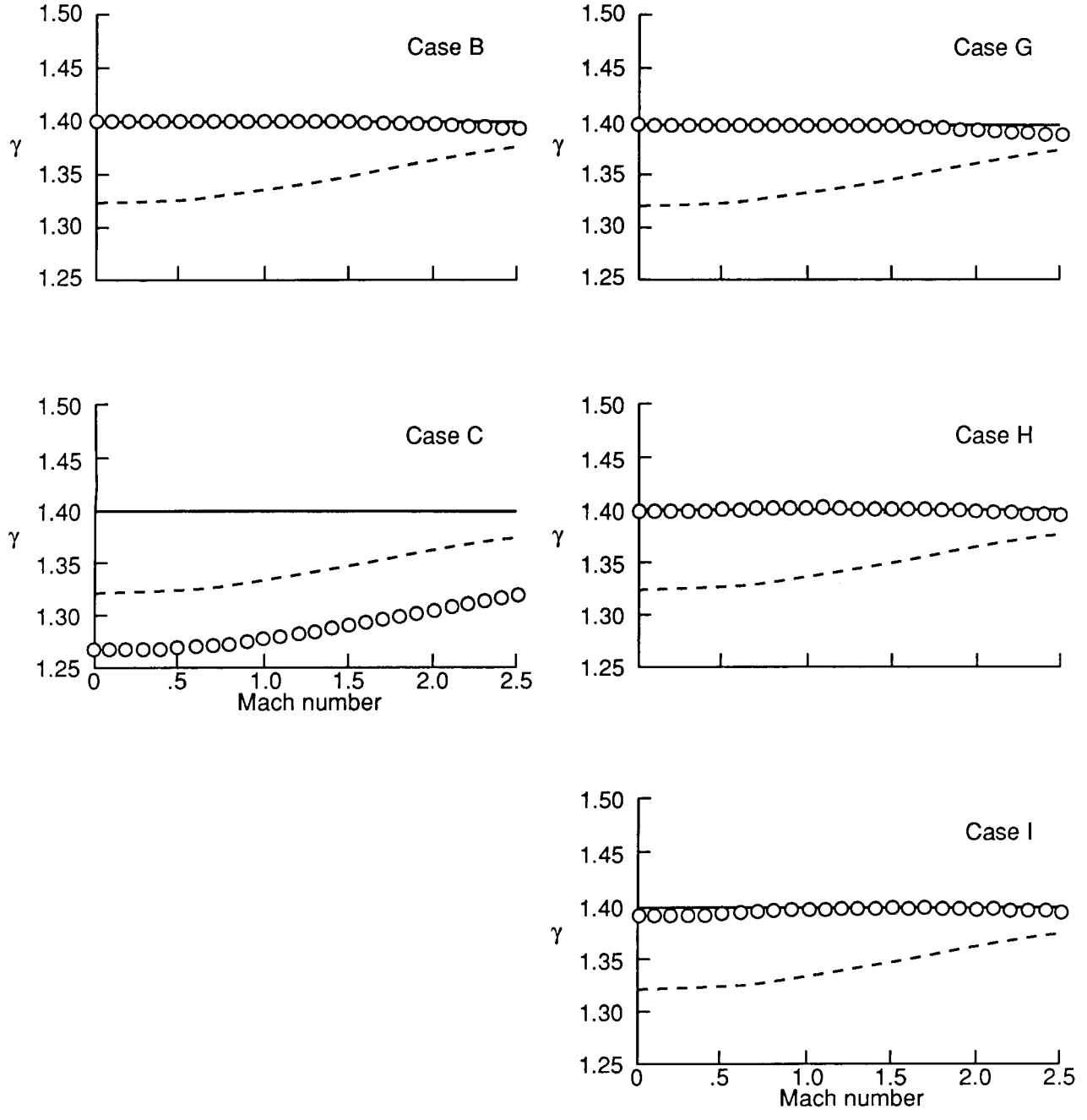

Figure 5. Variations of ratio of specific heats in isentropic expansions. (Curves for real turbojet exhaust gas are indicated by dashed lines.)

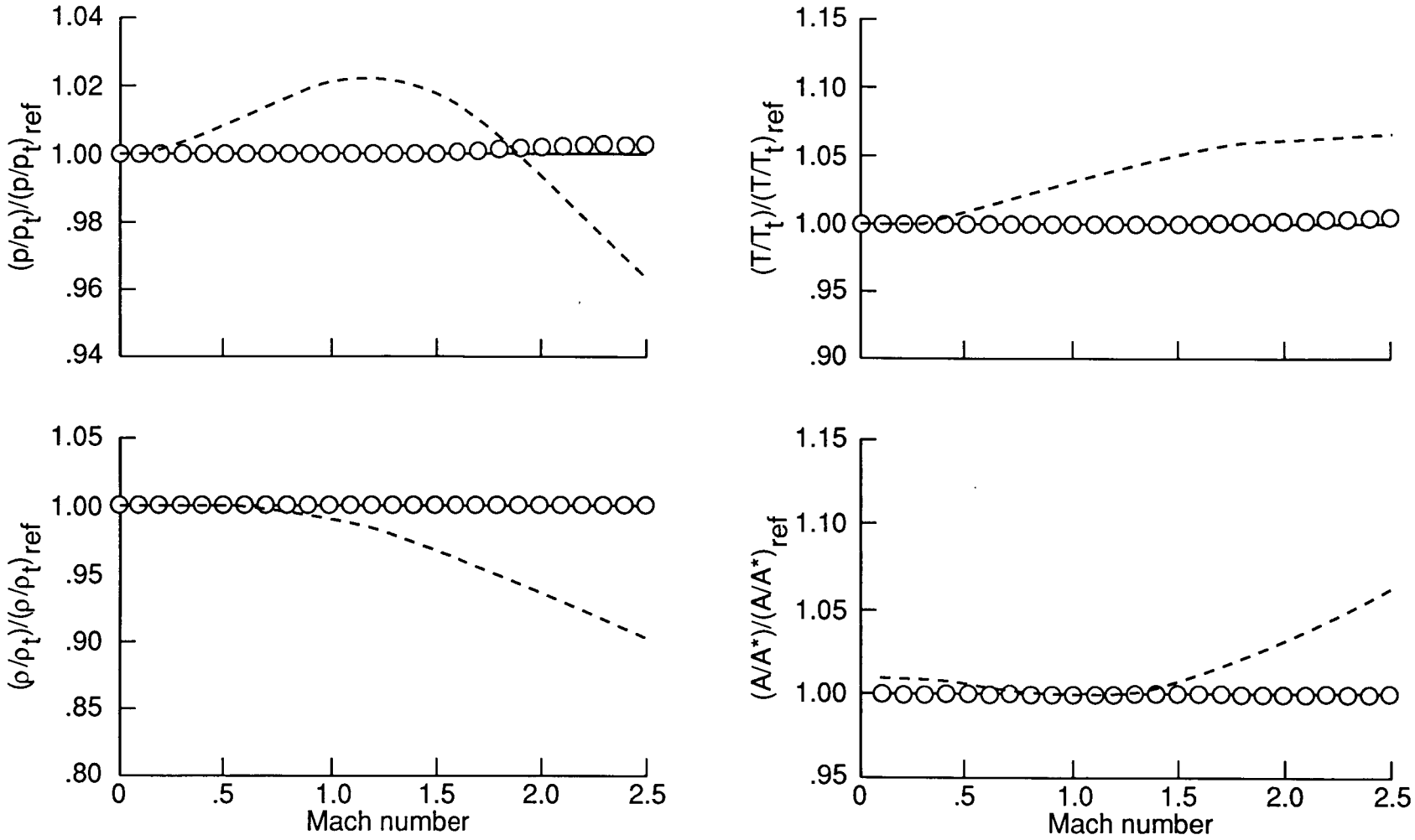

(a) Case B: Air; $p_{t,j} = 4.0$ bar; $T_{t,j} = 300$ K.

Figure 6. Variations of flow properties in isentropic expansions. (Curves for real turbojet exhaust gas are indicated by dashed lines.)

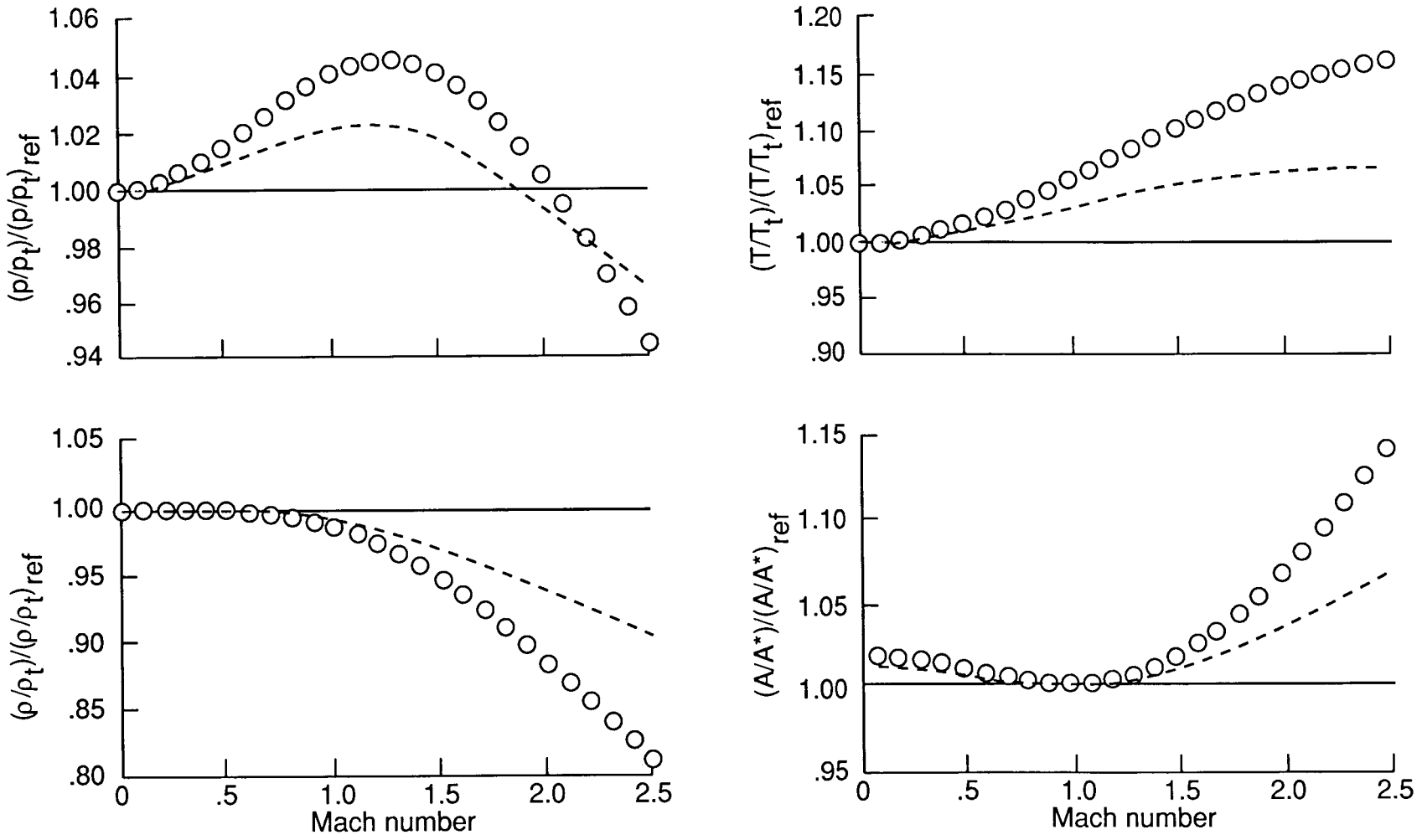

(b) Case C: $H_2O + O_2$; $p_{t,j} = 4.0$ bar; $T_{t,j} = 1000$ K.

Figure 6. Continued.

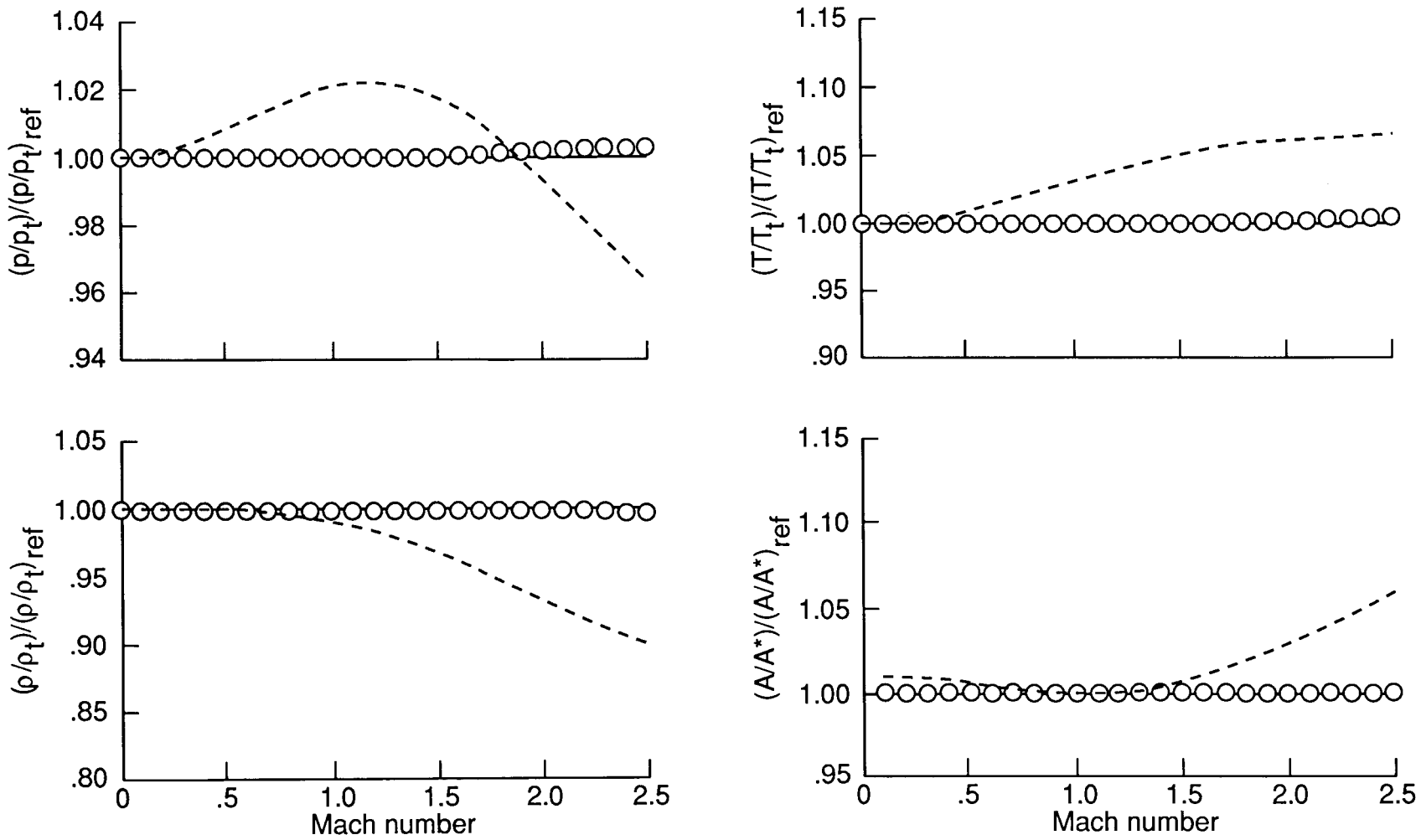

(c) Case G: N_2; $p_{t,j} = 8.0$ bar; $T_{t,j} = 333$ K.

Figure 6. Continued.

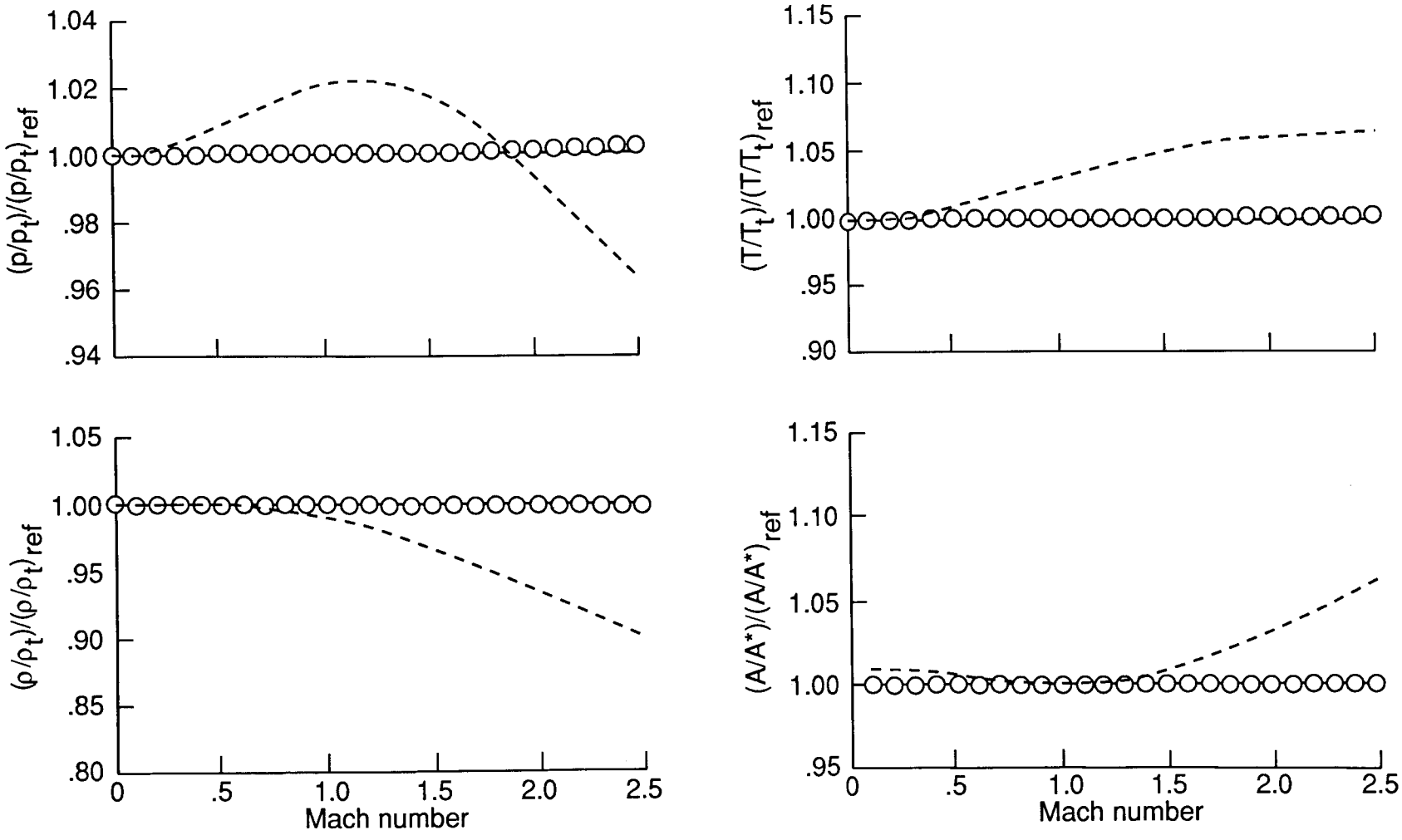

(d) Case H: N_2; $p_{t,j} = 12.0$ bar; $T_{t,j} = 417$ K.

Figure 6. Continued.

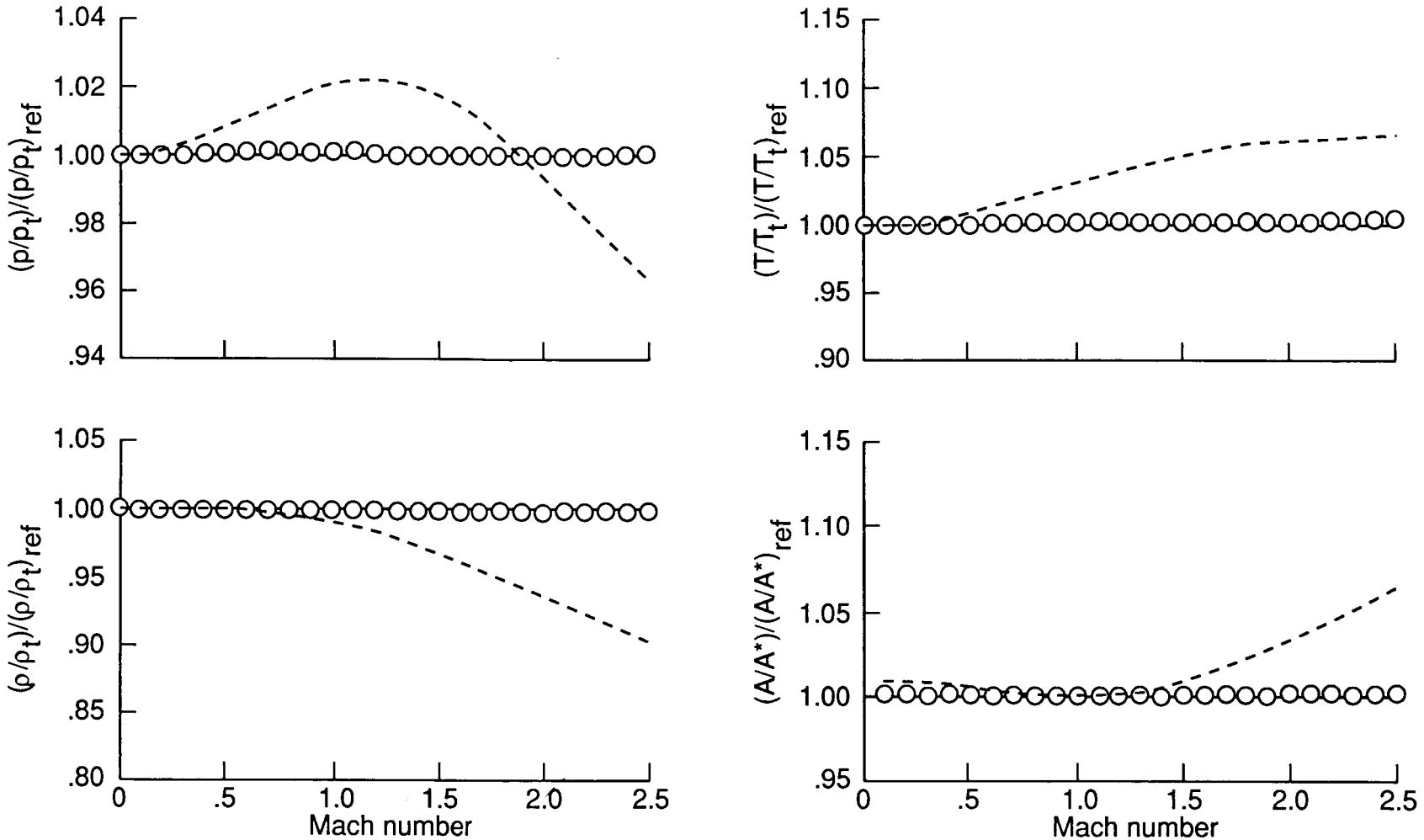

(e) Case I: N_2; $p_{t,j} = 16.0$ bar; $T_{t,j} = 500$ K.

Figure 6. Concluded.

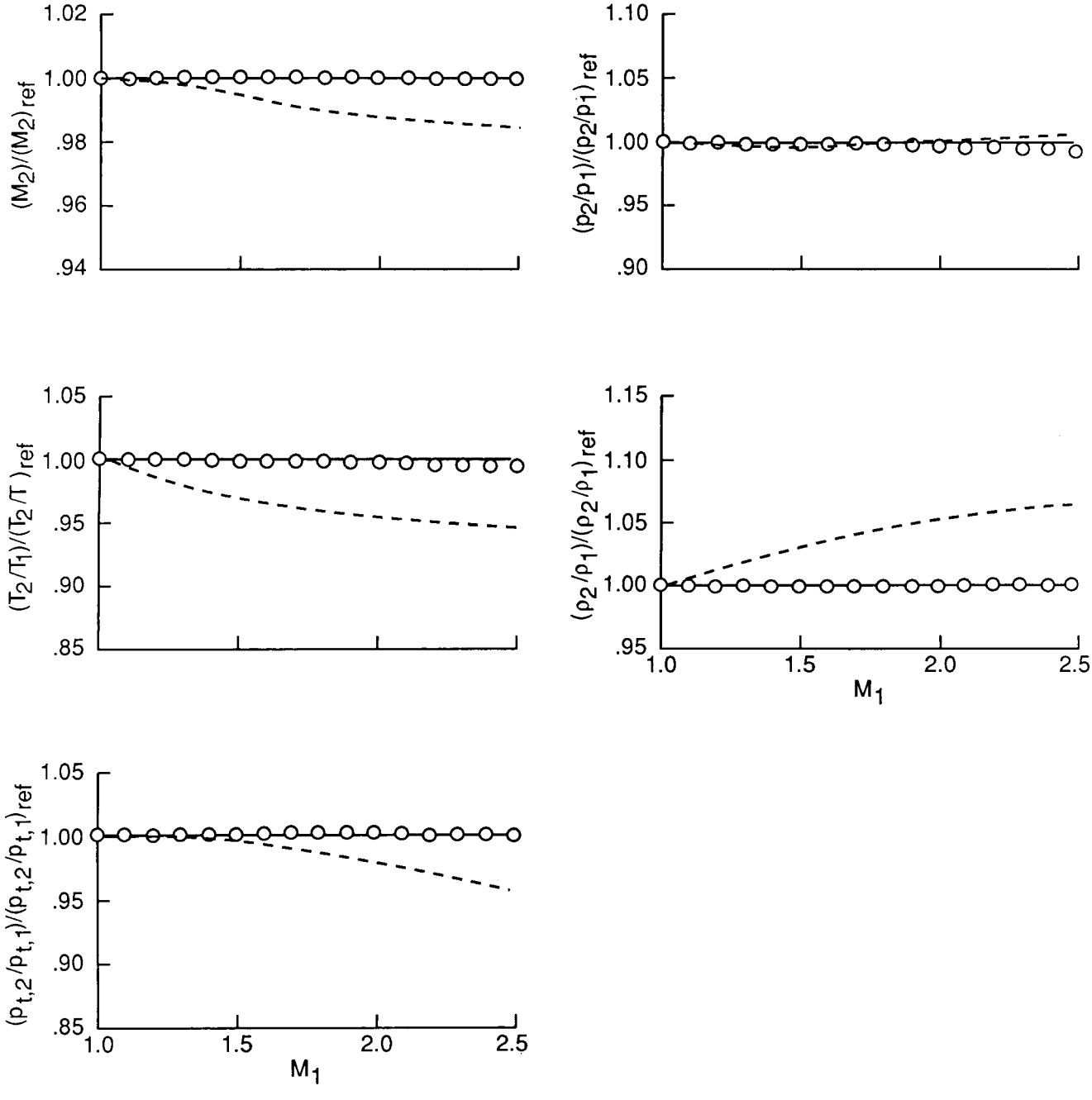

(a) Case B: Air; $p_{t,j} = 4.0$ bar; $T_{t,j} = 300$ K.

Figure 7. Variations of flow properties through normal shocks. (Curves for real turbojet exhaust gas are indicated by dashed lines.)

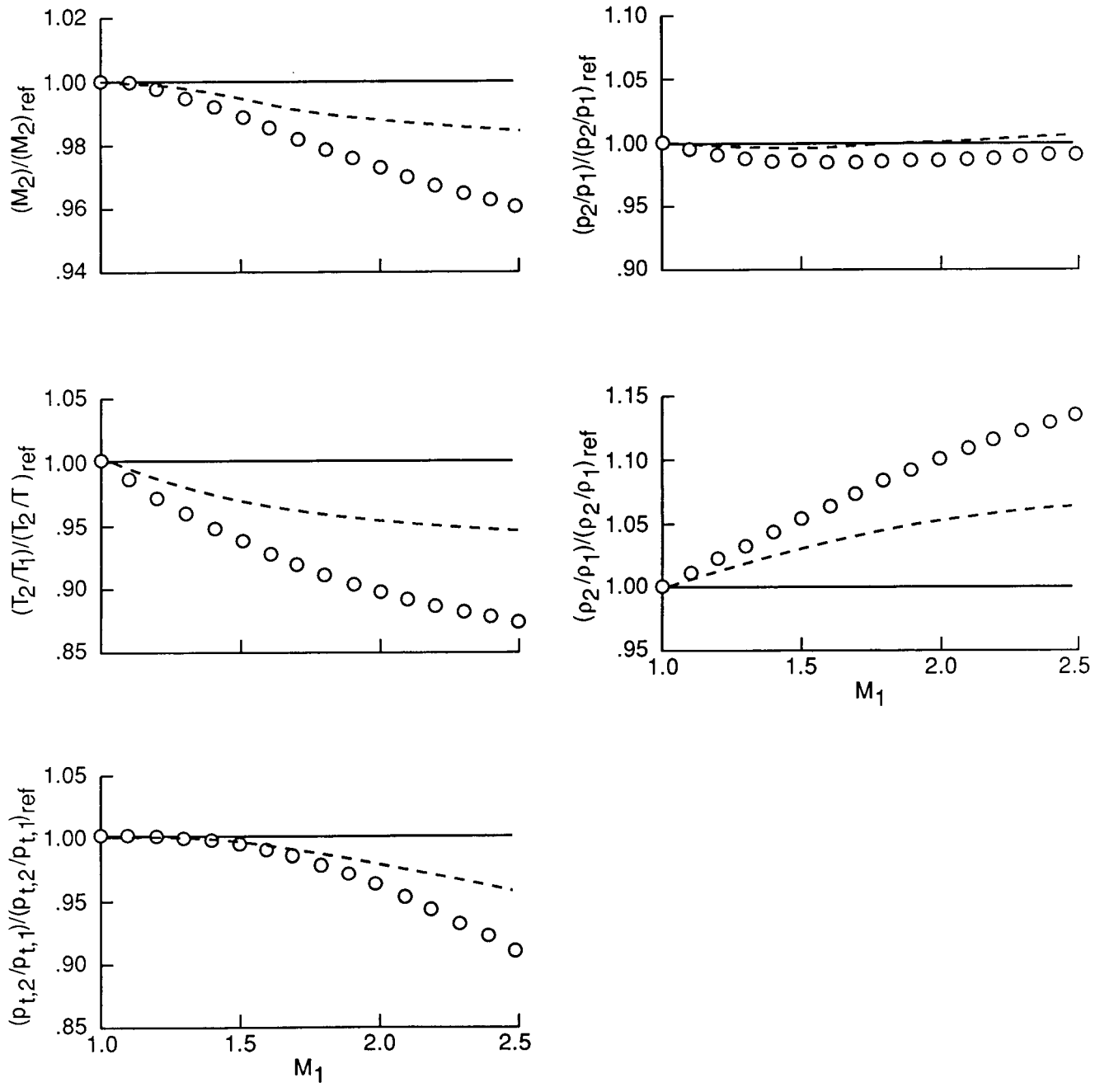

(b) Case C: $H_2O + O_2$; $p_{t,j} = 4.0$ bar; $T_{t,j} = 1000$ K.

Figure 7. Continued.

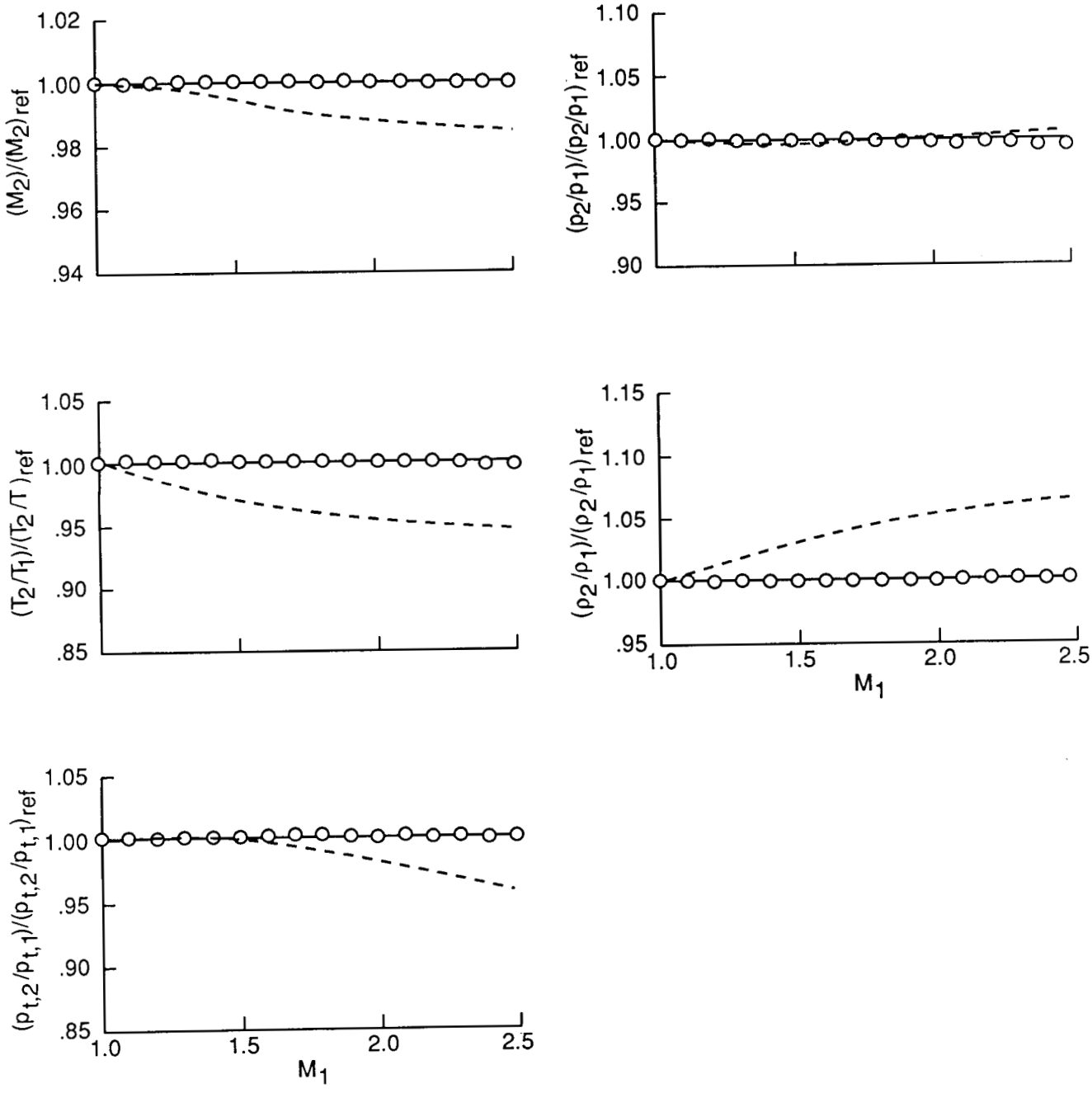

(c) Case G: N_2; $p_{t,j} = 8.0$ bar; $T_{t,j} = 333$ K.

Figure 7. Continued.

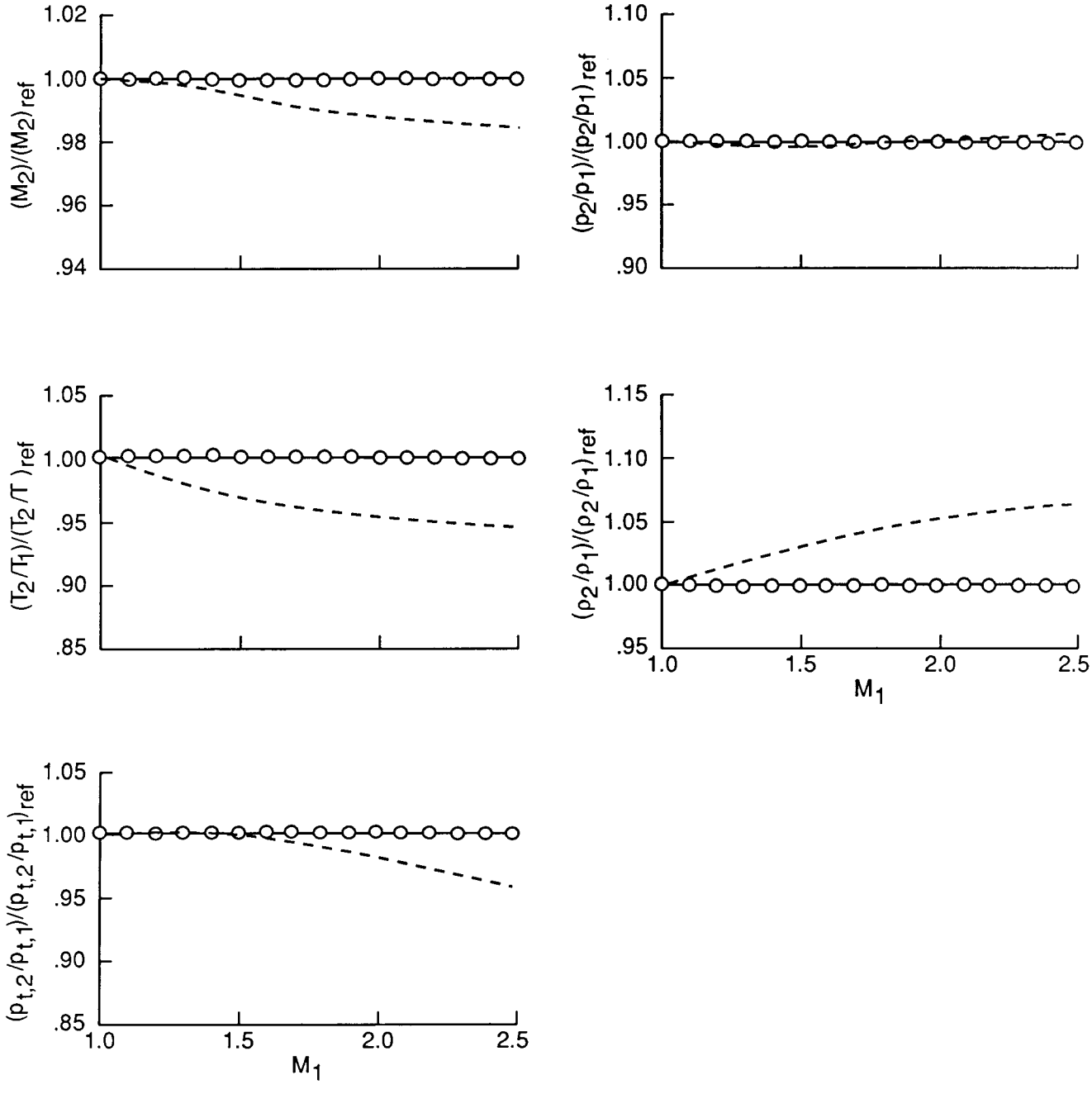

(d) Case H: N_2; $p_{t,j} = 12.0$ bar; $T_{t,j} = 417$ K.

Figure 7. Continued.

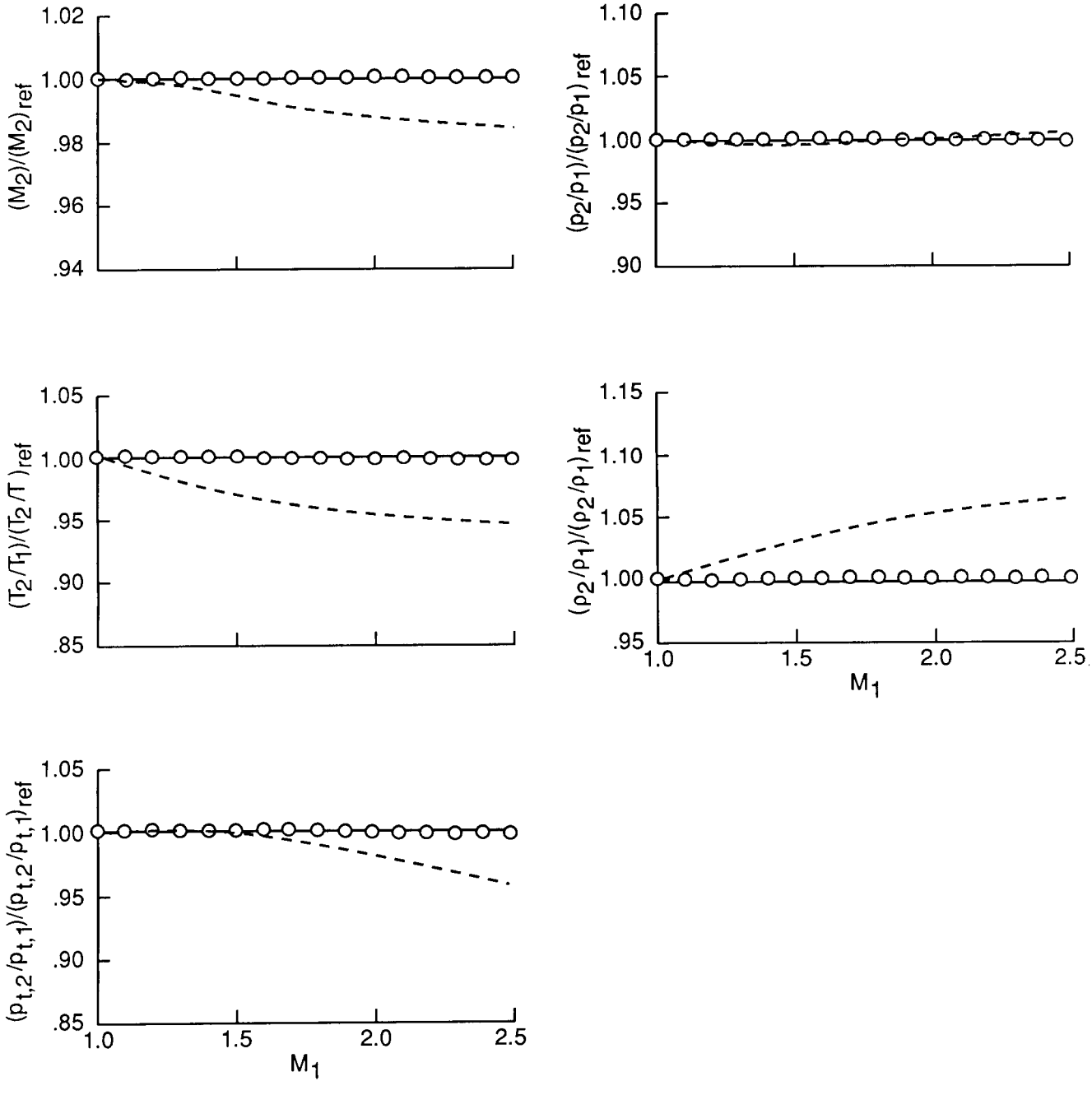

(e) Case I: N_2; $p_{t,j} = 16.0$ bar; $T_{t,j} = 500$ K.

Figure 7. Concluded.

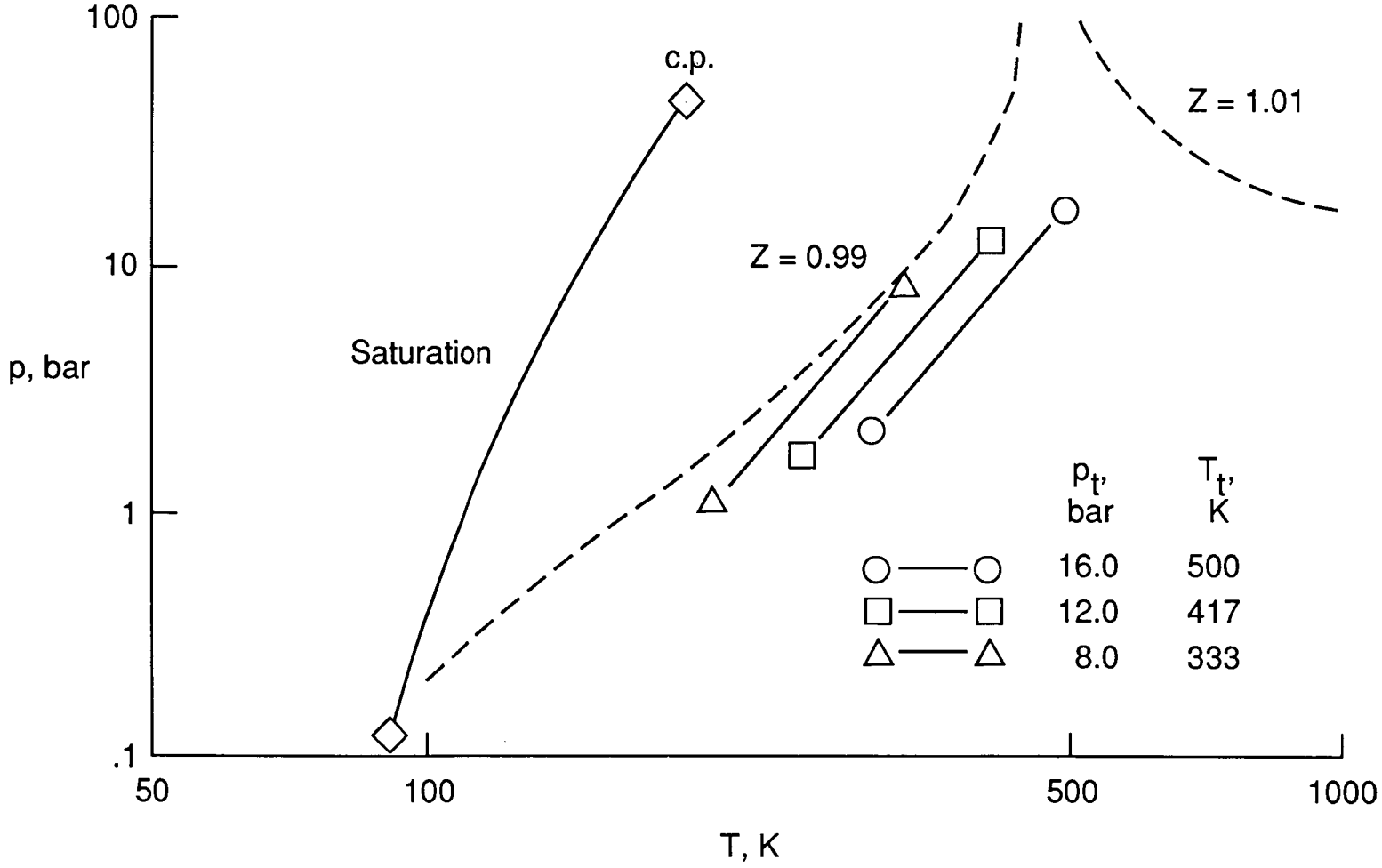

Figure 8. Isentropic expansions of methane gas.

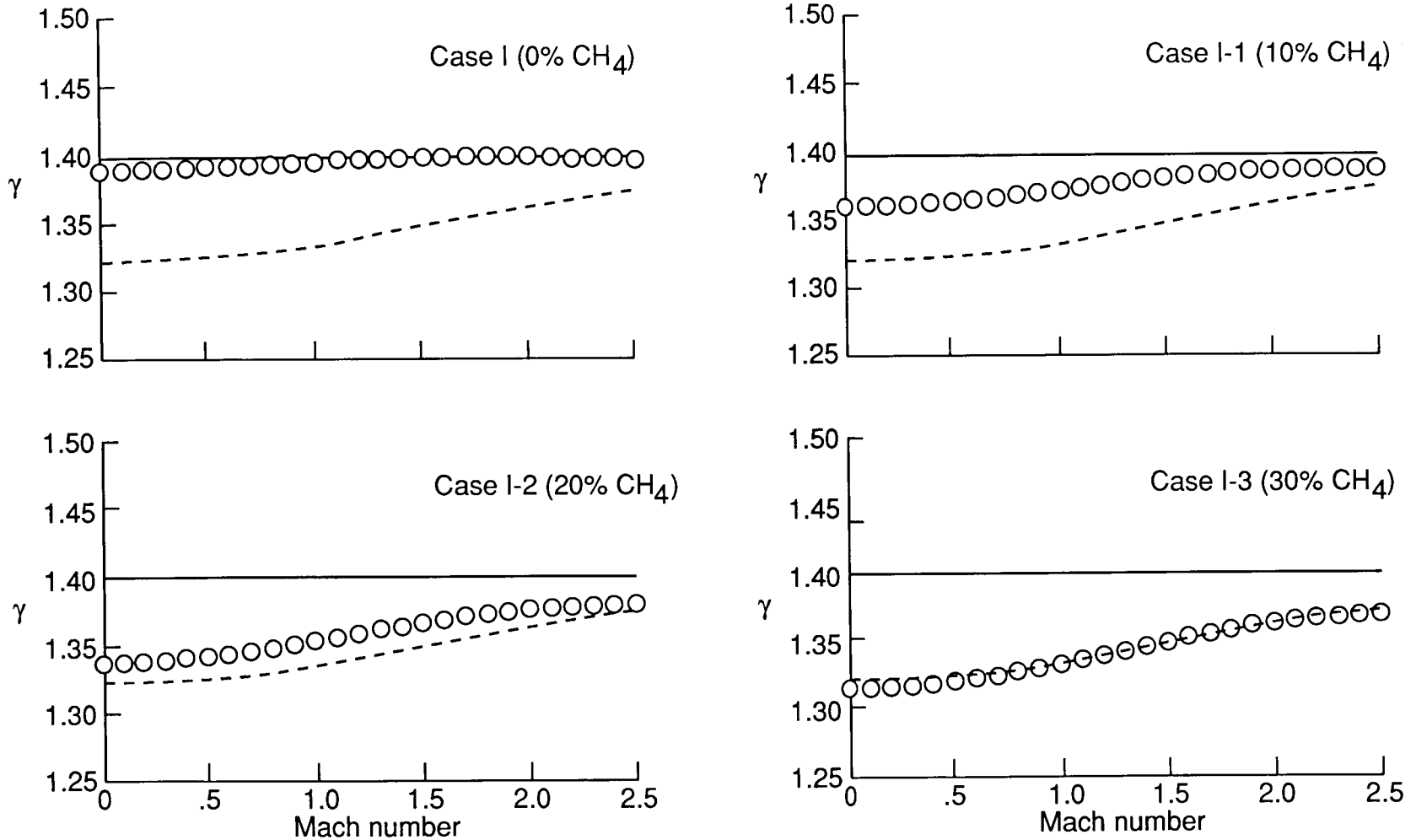

Figure 9. Ratio of specific heats for nitrogen-methane mixtures of various mole fractions (cases I to I-3, $T_{t,j} = 500$ K).

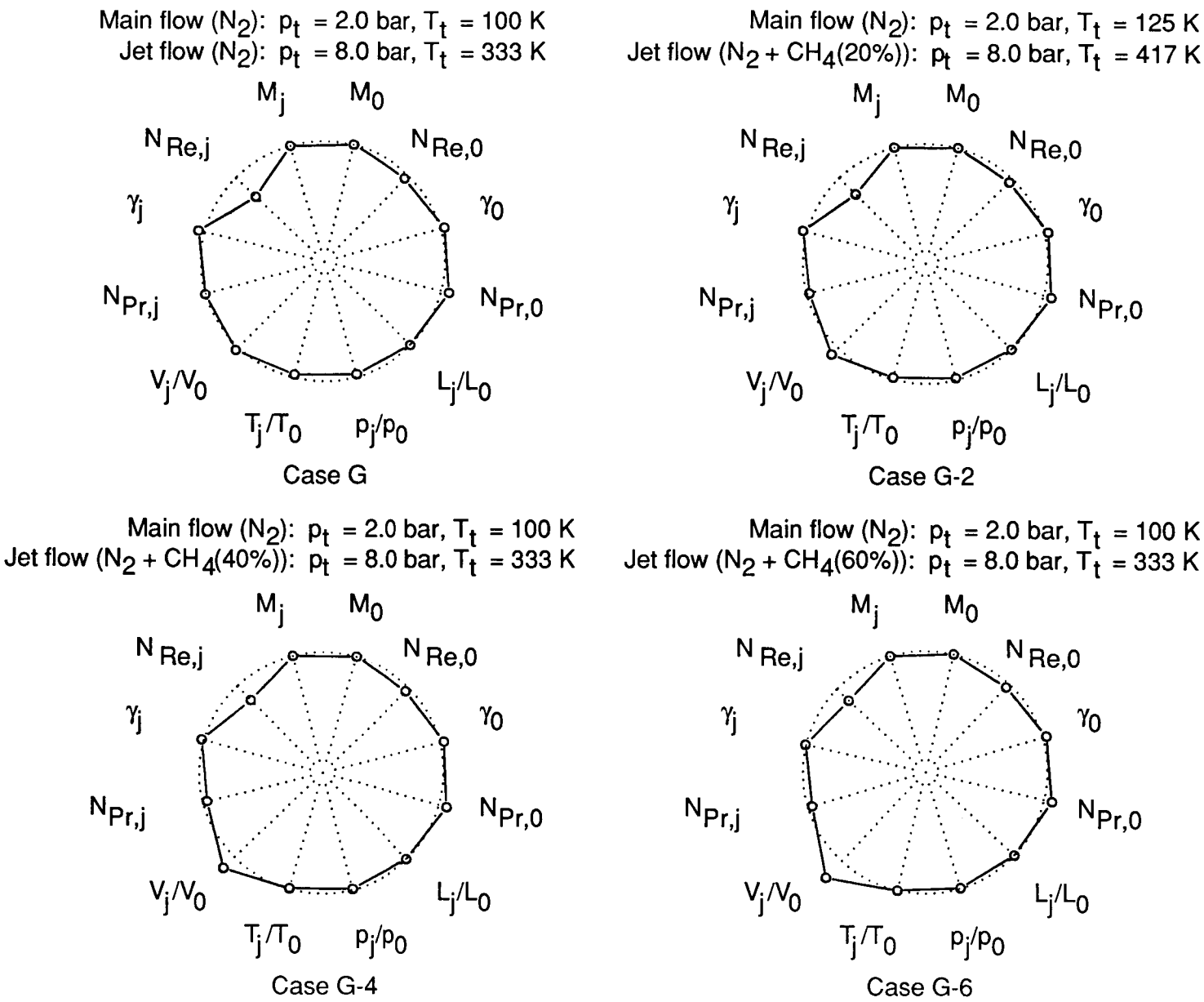

(a) Cases G, G-2, G-4, and G-6 ($T_{t,j}$ = 333 K).

Figure 10. Simulation capabilities of jet simulation techniques with nitrogen-methane mixture as jet gas.

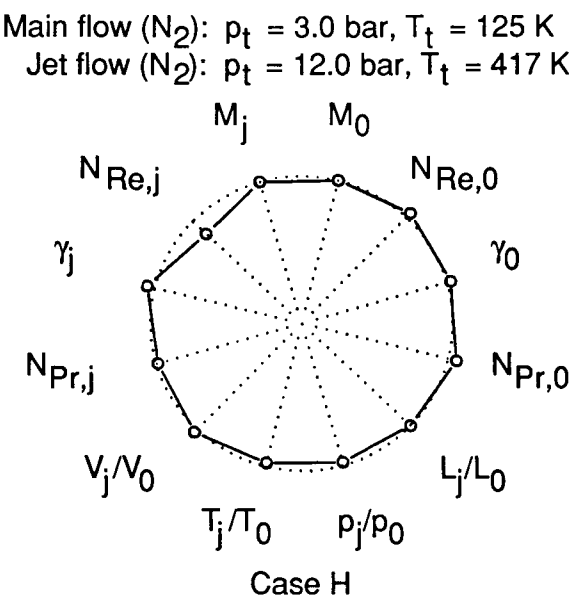

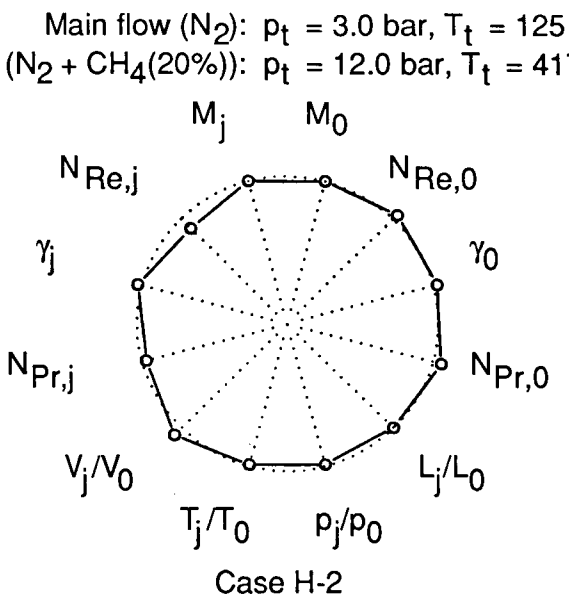

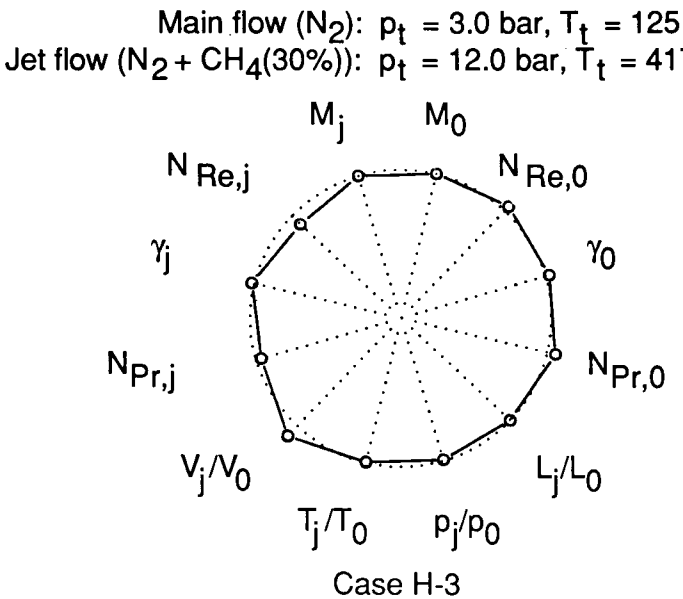

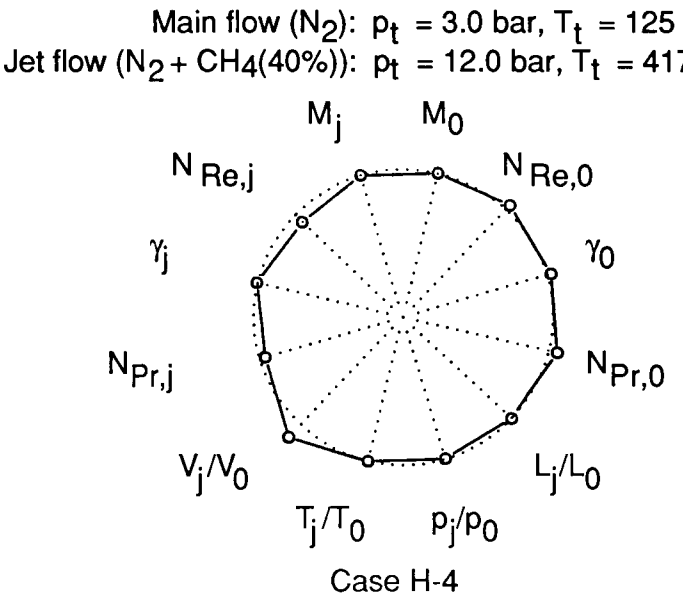

(b) Cases H, H-2, H-3, and H-4 ($T_{t,j}$ = 417 K).

Figure 10. Continued.

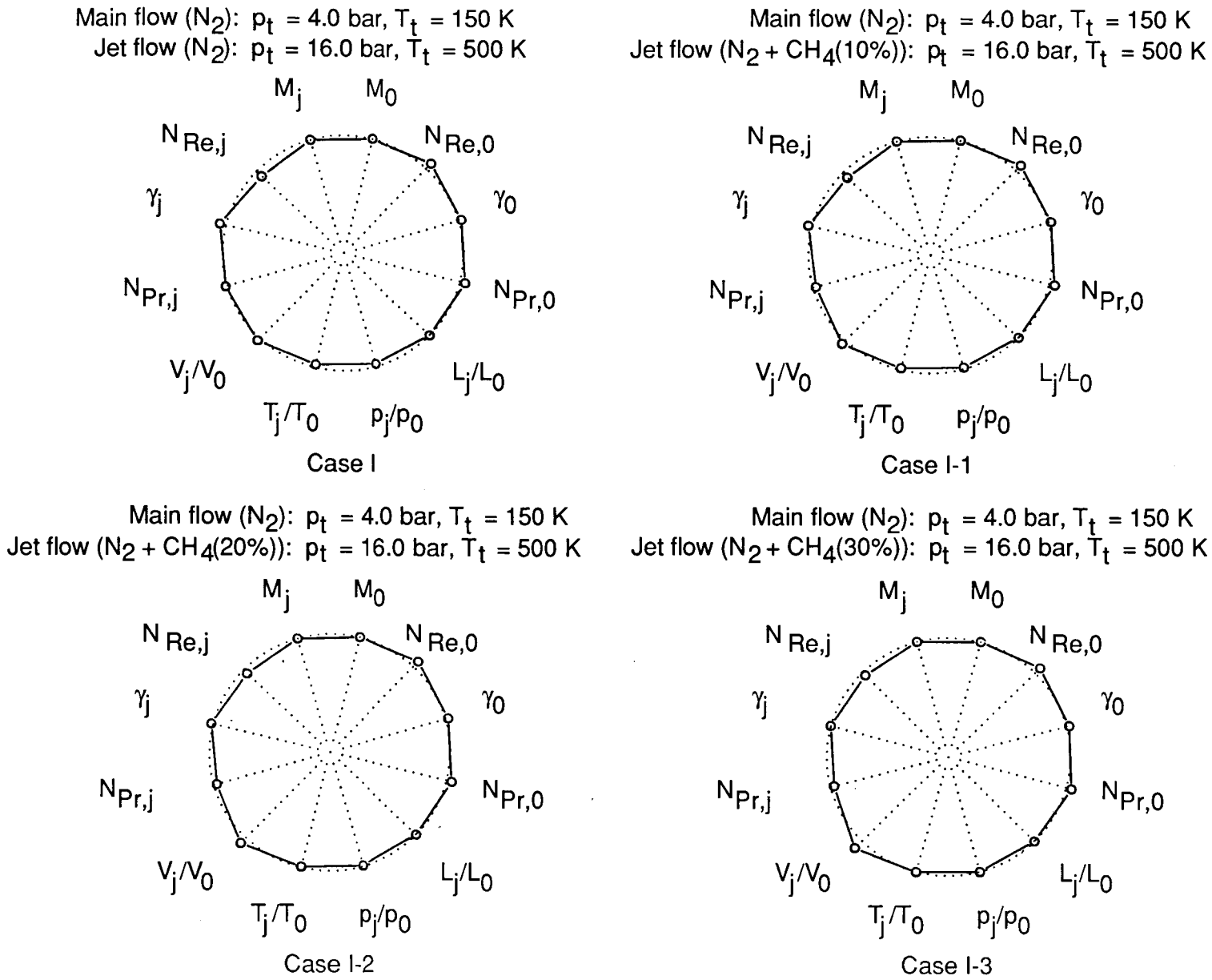

(c) Cases I, I-1, I-2, and I-3 ($T_{t,j}$ = 500 K).

Figure 10. Concluded.

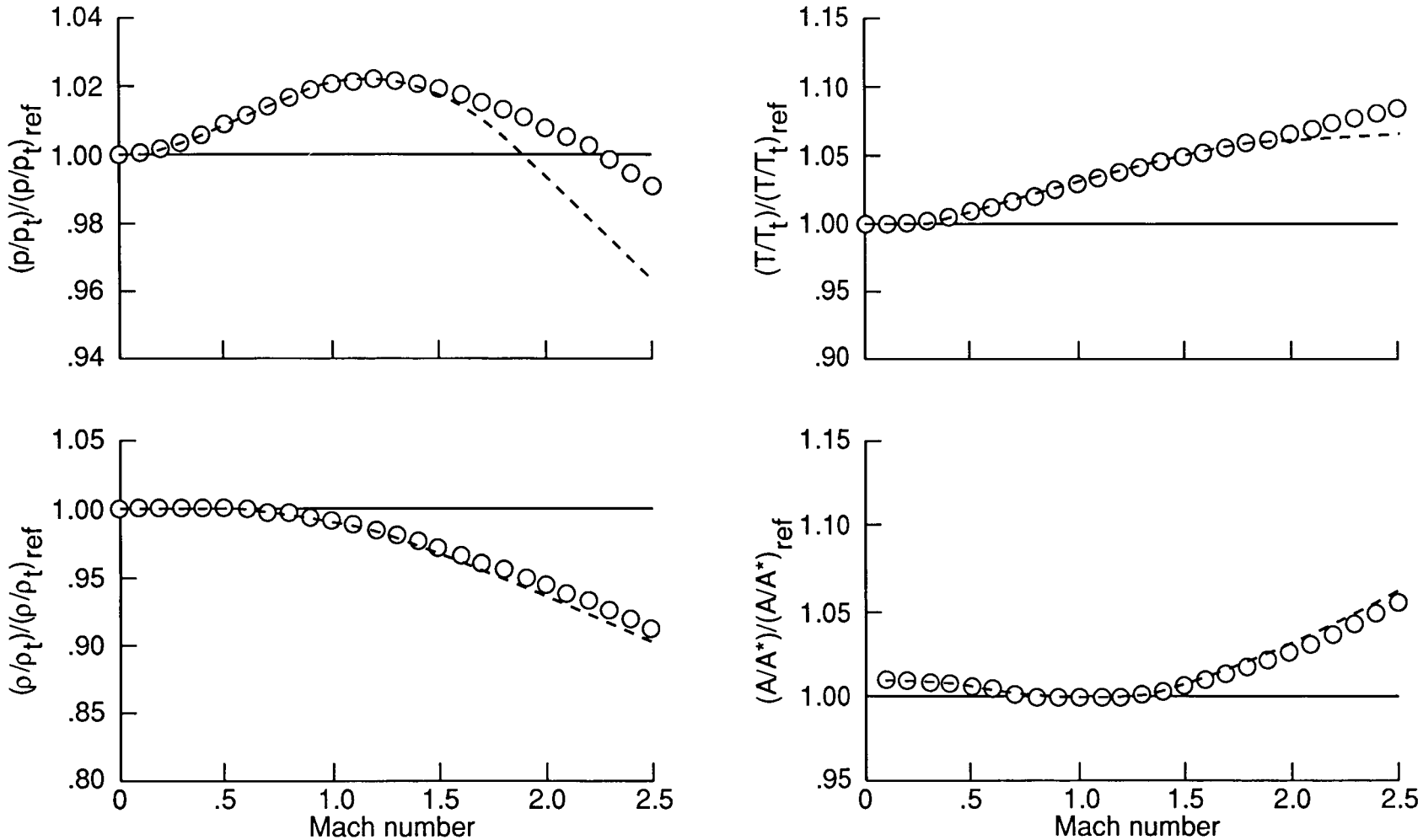

(a) Case G-6: N_2 + CH_4 (60%); $p_{t,j}$ = 8.0 bar; $T_{t,j}$ = 333 K.

Figure 11. Variations of flow properties in isentropic expansions with nitrogen-methane test gas. (Curves for real turbojet exhaust gas are indicated by dashed lines.)

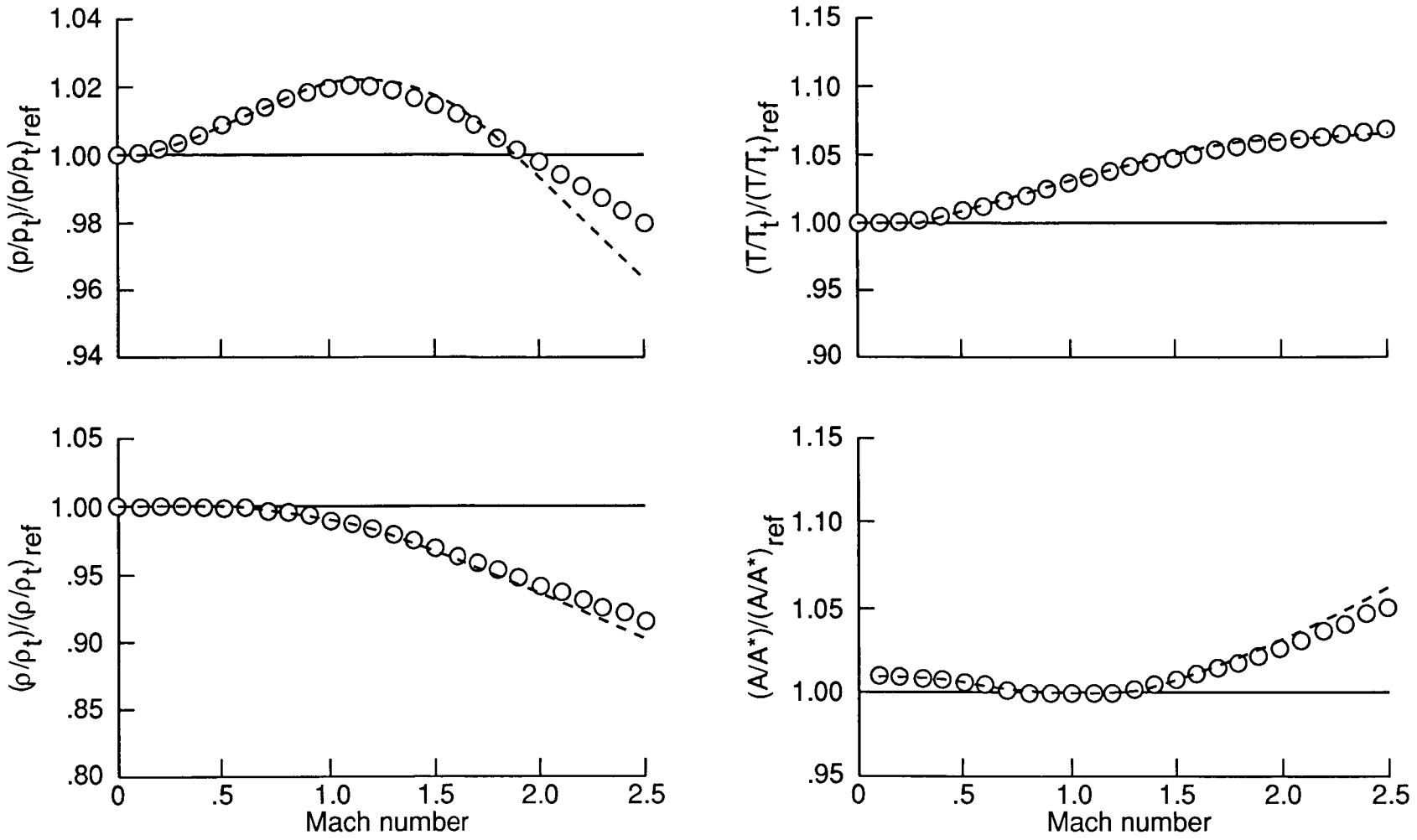

(b) Case H-4: N_2 + CH_4 (40%); $p_{t,j}$ = 12.0 bar; $T_{t,j}$ = 417 K.

Figure 11. Continued.

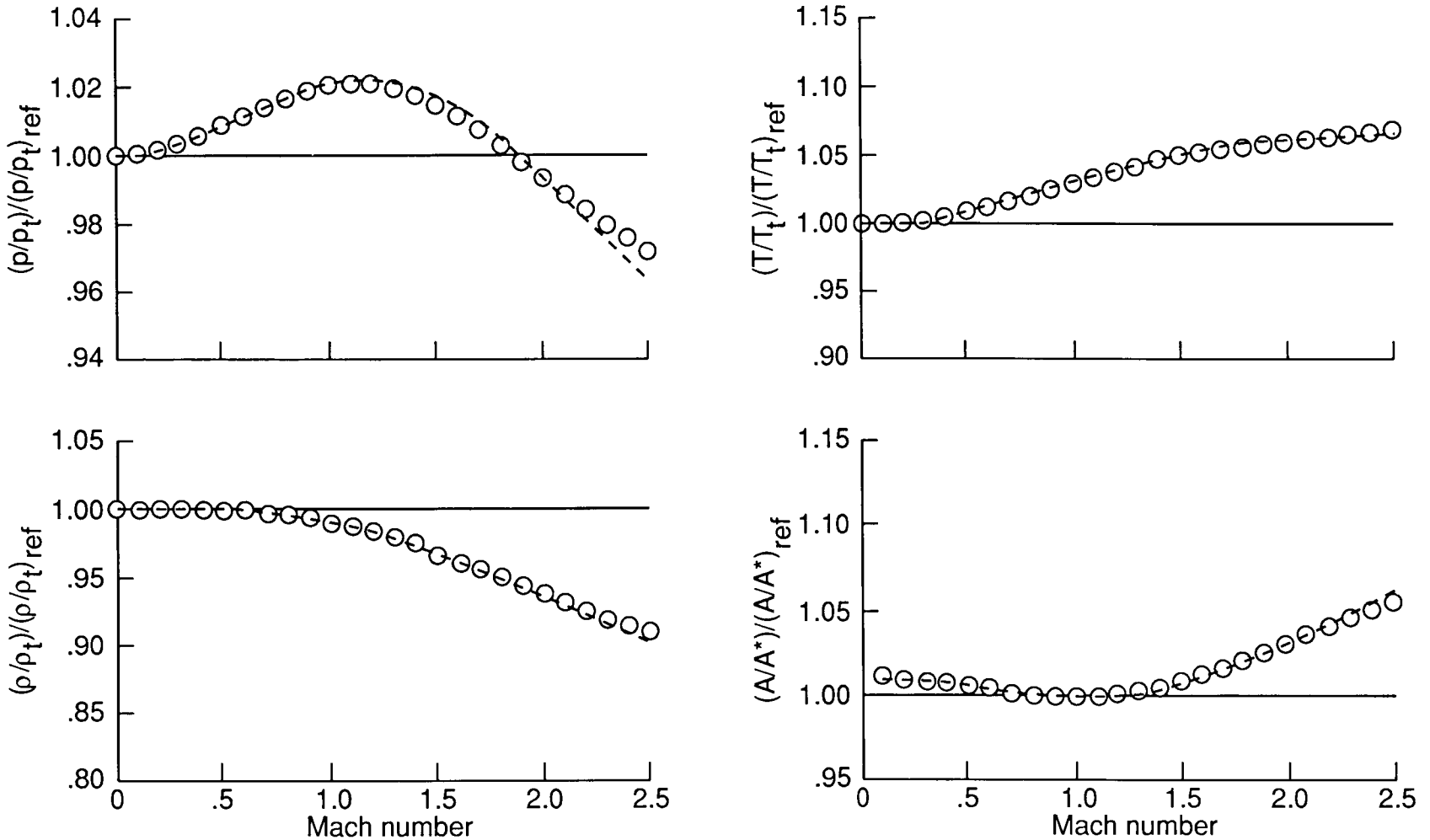

(c) Case I-3: N_2 + CH_4 (30%); $p_{t,j}$ = 16.0 bar; $T_{t,j}$ = 500 K.

Figure 11. Concluded.

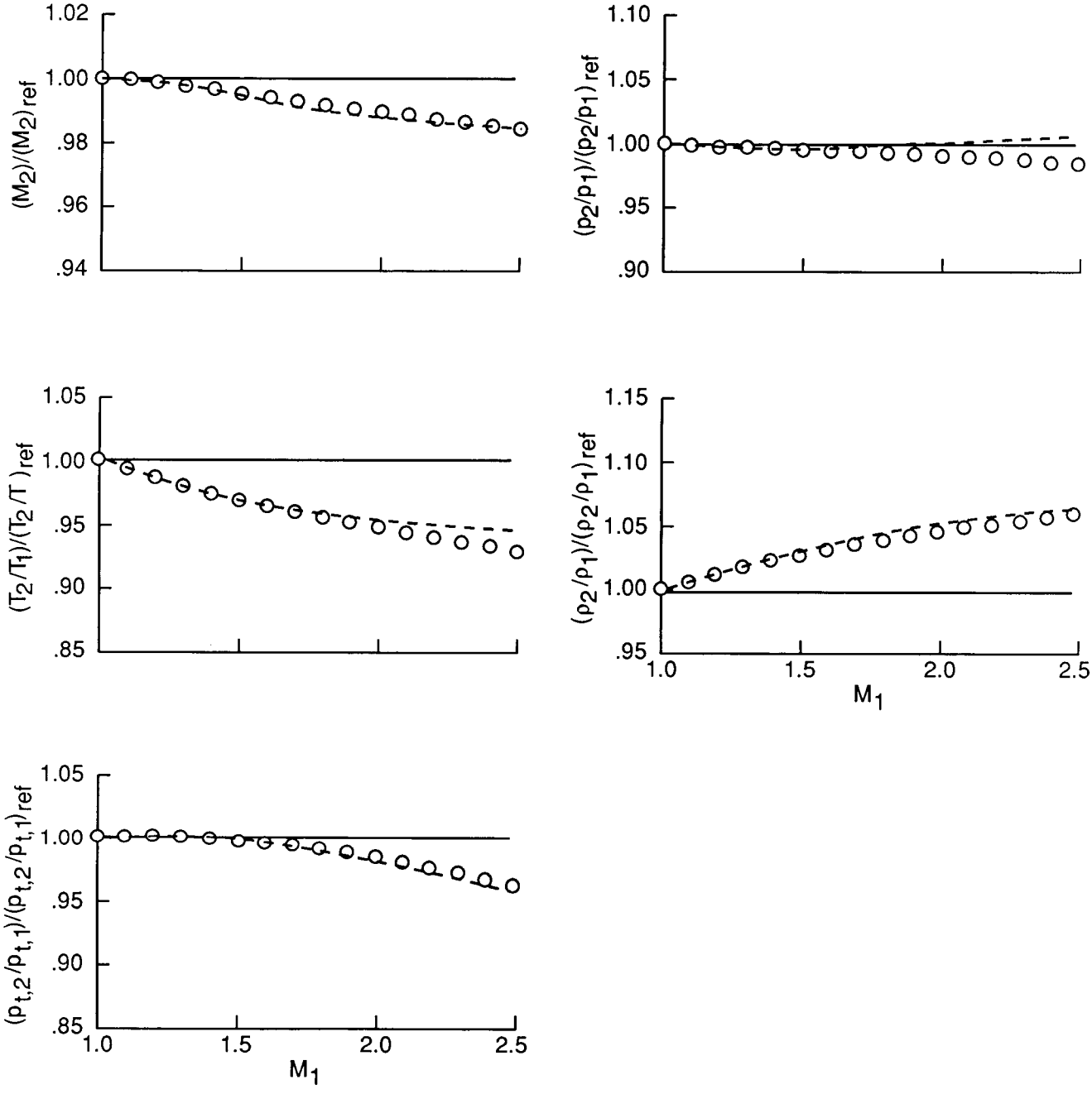

(a) Case G-6: N_2 + CH_4 (60%); $p_{t,j}$ = 8.0 bar; $T_{t,j}$ = 333 K.

Figure 12. Variations of flow properties through normal shocks with nitrogen-methane test gas. (Curves for real turbojet exhaust gas are indicated by dashed lines.)

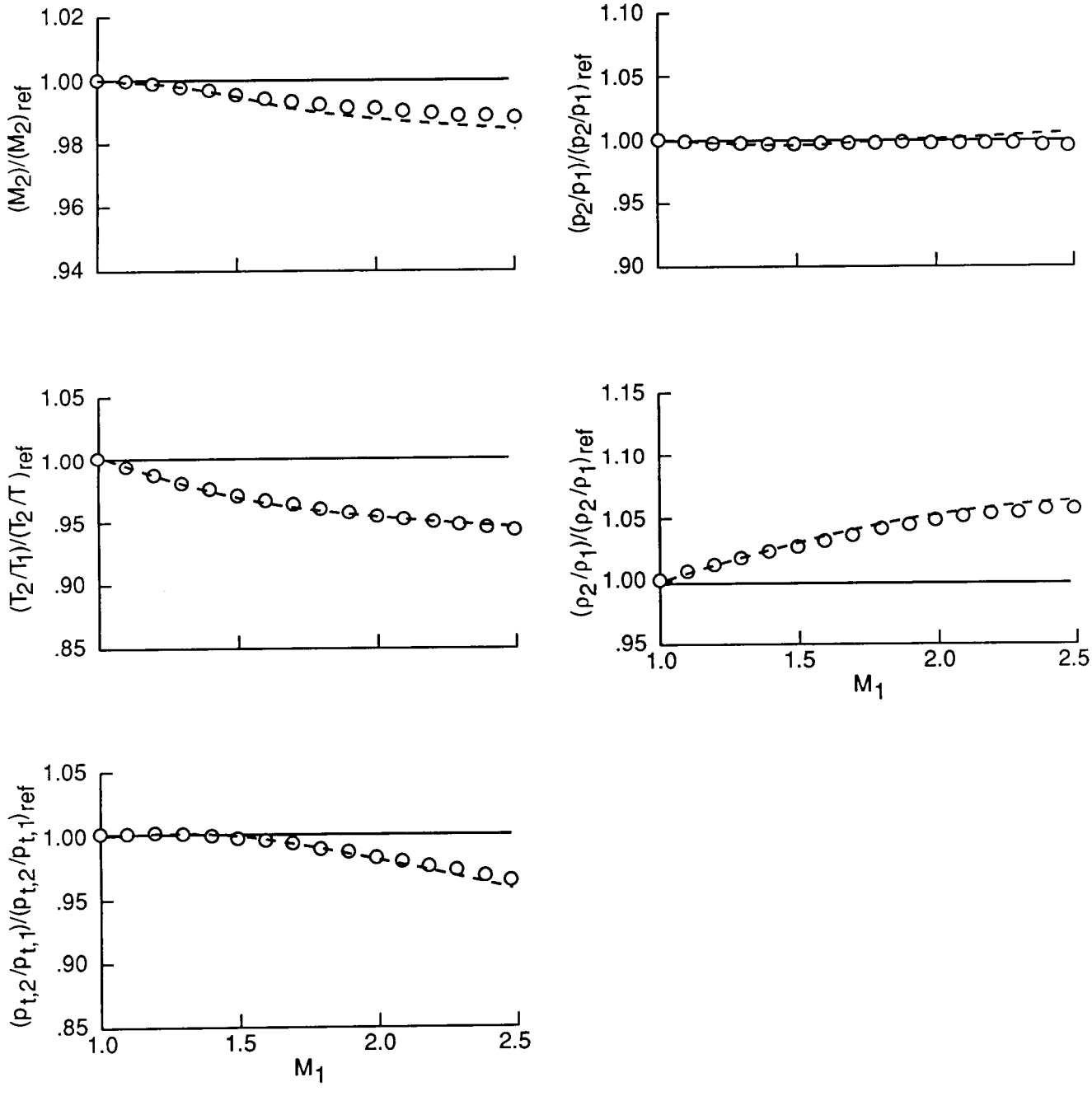

(b) Case H-4: N_2 + CH_4 (40%); $p_{t,j}$ = 12.0 bar; $T_{t,j}$ = 417 K.

Figure 12. Continued.

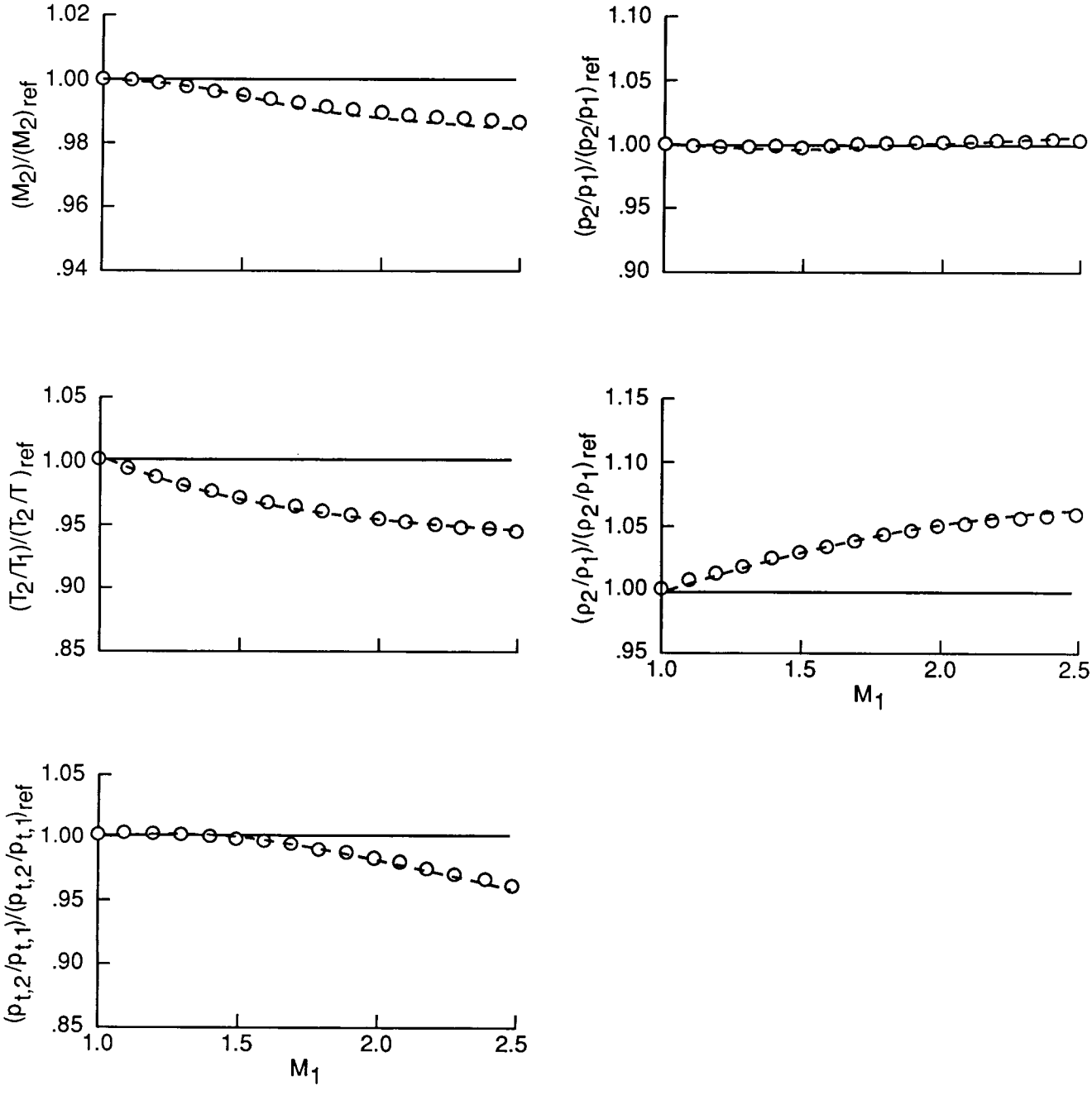

(c) Case I-3: N_2 + CH_4 (30%); $p_{t,j}$ = 16.0 bar; $T_{t,j}$ = 500 K.

Figure 12. Concluded.

NASA
National Aeronautics and Space Administration

Report Documentation Page

1. Report No.	2. Government Accession No.	3. Recipient's Catalog No.
NASA RP-1220		

4. Title and Subtitle	5. Report Date
Hot-Jet Simulation in Cryogenic Wind Tunnels	July 1989
	6. Performing Organization Code
7. Author(s)	8. Performing Organization Report No.
Keisuke Asai	L-16564
9. Performing Organization Name and Address	10. Work Unit No.
NASA Langley Research Center Hampton, VA 23665-5225	505-61-01-01
	11. Contract or Grant No.
12. Sponsoring Agency Name and Address	13. Type of Report and Period Covered
National Aeronautics and Space Administration Washington, DC 20546-0001	Reference Publication
	14. Sponsoring Agency Code

15. Supplementary Notes

Keisuke Asai: Visiting research engineer from the National Aerospace Laboratory, Tokyo, Japan.

16. Abstract

In order to evaluate hot-jet simulation capabilities in cryogenic wind tunnel testing, simple theoretical calculations have been performed. The similarity parameters, isentropic flow properties, and normal shock relations were calculated for a variety of jet simulation techniques. The results were compared with those estimated for a full-scale flight condition. It has been shown that cryogenic wind tunnel testing provides an opportunity for the most accurate hot-jet simulation. By using compressed nitrogen gas at ambient or moderately elevated temperatures as a jet gas, almost all the relevant similarity parameters, including the jet temperature and velocity ratios and the Reynolds numbers, could be set to full-scale flight values. The only exception was the ratio of specific heats for jet flow. In an attempt to match the ratio of specific heats for the turbojet flow, gases other than pure nitrogen were considered. It was found that a nitrogen and methane mixture at moderately elevated temperatures behaved like the real combustion gas. With this mixture used as a jet gas, complete simulation of the full-scale turbojet exhaust became possible in cryogenic wind tunnels.

17. Key Words (Suggested by Authors(s))	18. Distribution Statement
Hot-jet simulation Cryogenic wind tunnel Reynolds numbers	Unclassified—Unlimited Subject Category 05

19. Security Classif. (of this report)	20. Security Classif. (of this page)	21. No. of Pages	22. Price
Unclassified	Unclassified	46	A03

For sale by the National Technical Information Service, Springfield, Virginia 22161-2171